The 61st Israel Annual Conference on

Aerospace Science

For over six decades, IACAS is an annual event on the calendar of the aerospace community in Israel, and arouses a great deal of interest abroad. Taking part in this yearly event are engineers, scientists, and experts in the field of aeronautics and astronautics, representing well-known local aerospace agencies and industries, as well as participants from major research centers worldwide.

The two-day conference covers new research, presents up-to-date technology, and provides a forum for exchanging new ideas.

Chair, Organizing Committee

Ms. Gila Ghilai, Israel Aerospace Industries

Chair, Program Committee

Assoc. Prof. Avshalom Manela,
Faculty of Aerospace Engineering, Technion

ORGANIZING COMMITTEE

Gila Ghilai, Chair	Israel Aerospace Industries
Shlomo Barenholtz	Israel Aerospace Industries
Daniel Choukroun	Ben-Guryon University of the Negev
Agnes Cohen	ELBIT Systems
Beni Davidor	Civil Aviation Authority
Yoav Emek	RAFAEL
Hana Flum, Secretary	Technion
Alon Gany	Technion
Dan Givoli	Technion
Michael Iovnovich	Israeli Air Force
Yuval Levy	Israeli CFD Center
Daniella Raveh, Treasurer	Technion
Tomer Rokita	RAFAEL
Avi Seifert	Tel-Aviv University
Tal Shakked	Israel Aerospace Industries
Tal Shima, Dean, Aerospace Eng.	Technion
Tal Yehoshua	Israeli Ministry of Defense
Israel Zeierman	ISAA

PROGRAM COMMITTEE

Avshalom Manela, Chair	Technion
Haim Abramovich	Technion
Rimon Arieli	Technion
Shai Arogeti	Ben-Gurion University of the Negev
Beni Chukurel	Technion
Moshe Idan	Technion
Gil Iosilevskii	Technion
Ian Jacobi	Technion
Moti Karpel	Technion
Amiram Leitner	RAFAEL
Yuval Levy	Israeli CFD Center
Danny Michaels	Technion
David Mishne	Technion
Daniella Raveh	Technion
Eran Sher	Technion
Haim Weiss	Rafael
Martin Weiss	Technion
Gil Yudilevitch	Technion
Daniel Zelazo	Technion

CONFERENCE PRODUCTION MANAGER

Tal Rappoport	Technion

WeL2T1 | Hall A

Guidance, Navigation, and Control - II

Chair: **Daniel Choukroun** — Ben-Gurion University of the Negev

16:25-16:50 | WeL2T1.1

Robust Trajectory Tracking of a Multicopter Using Linear Quadratic Differential Game Approach

Bhargav Jha — Technion
Ujjwal Gupta — Georgia Institute of Technology
Vladimir Turetsky — Ort Braude College
Tal Shima — Technion

16:50-17:15 | WeL2T1.2

Optimal Impact-Time Control Guidance with Terminal Angle Constraint Using Quadratic Kinematics Approximation

Gleb Merkulov — Technion
Martin Weiss — Technion
Tal Shima — Technion

17:15-17:40 | WeL2T1.3

Analytical Description of Three-Dimensional Reachable Set for Dubins Car

Valery S. Patsko — Institute of Mathematics and Mechanics, Ural Branch of Russian Ac
Andrey Anatol'evich Fedotov — Institute of Mathematics and Mechanics, Ural Branch of Russian Ac

17:40-18:05 | WeL2T1.4

State Dependent Coefficient Form Based Solution of the Quadratic Optimal Control for Nonlinear Systems

Ilan Rusnak — RAFAEL
Maital Levy — Technion

Analytical description of three-dimensional reachable set for Dubins car

Valerii S. Patsko* and Andrey A. Fedotov†
Krasovskii Institute of Mathematics and Mechanics, Ekaterinburg, Russia

The Dubins car is a model of motion, in which the scalar control u determines the instantaneous angular velocity of rotation. The paper considers a symmetric variant of the constraints $u \in [u_1, u_2]$, where $u_1 = -u_2$, $u_2 = 1$. We study the three-dimensional reachable set at a given instant $t_f > 0$. An analytical description of two-dimensional sections of the set w.r.t. the angular coordinate φ is given. The boundary of each φ-section is formed with the help of a certain set of curves obtained using the Pontryagin maximum principle. This set includes the arcs of circles, as well as, the involutes of circles. The symmetry property of each φ-section w.r.t. a certain straight line is established. A classification of possible types of the φ-sections is proposed. The greatest difficulty is presented by analysis of the case with non-simply connected φ-sections. The range of values φ and t_f, at which the φ-sections are non-simply connected, is indicated. Due to the large size of the paper, proofs of many auxiliary statements have been omitted.

Introduction

The mathematical "Dubins car" is a model of controllable motion, in which two phase variables x, y are the coordinates of a point geometric position in the plane, the third variable φ is the angle formed by the velocity vector with the positive direction of the axis x. The value of the linear velocity is considered to be constant and equal to 1. The scalar control u has the sense of the angular velocity of rotation (or, equivalently, the instantaneous radius of turn) and is restricted by the constraint $u \in [-1, 1]$.

The name of the model is related to work [1], in which L. Dubins established the properties of curves of the minimal length (with a radius of curvature bounded from below) that connect two points in the plane with the specified exit and entry directions. It corresponds to the time-optimal problem for an object moving at the constant speed and rotation radius restricted from below. The results obtained by L. Dubins have been reproven and supplemented with the help of the Pontryagin maximum principle in [2, 3].

Speaking about the previous history of similar problems, we should note article [4] by A.A. Markov, in which he considered four mathematical problems associated with the design of railways. In 1951, R. Isaacs, while working for the Rand Corporation, submitted his first report [5] on the theory of differential games, in which he posed and outlined the solution to the "homicidal chauffeur" problem. It was R. Isaacs who first began to call the described controllable object with the word "car".

This model (often referred to as the "simplified unicycle") is used when considering aircraft motions in the horizontal plane with the constant speed and small bank angles

*Leading Researcher, patsko@imm.uran.ru.
†Senior Researcher, andreyfedotov@mail.ru.

(see, e.g., [6, Chapter 4, Section 8.4], [7]). Such model is also applied for a simplified description of motion of controllable wheeled "bogies" [8] and autonomous underwater vehicles [9]. The list of meaningful problems in the plane, the mathematical description of which (after some transformations) is reduced to the Dubins model, is available in book [10].

The literature devoted to solving specific control problems using the Dubins car is huge. The most popular are various variants of the time-optimal problem [11–16] that includes problems with phase constraints. The time-optimal problems with the requirement of passing through the given points are considered in works [17–20]. Synthesis of the time-optimal control for the Dubins car under the standard three-dimensional termination condition is presented in paper [7]. The problems of possibility of elongation curves solving the time-optimal problem with the three-dimensional termination condition for a certain period of time are considered in [21]. In some works (e.g., [22–25]), solutions of pursuit problems close to game problems are investigated where the pursuer has the dynamics of the Dubins car. Some papers study connection between the standard time-optimal problem of object transferring to a given set in the space of geometric coordinates with the solution of the "homicidal chauffeur" differential game [26–28].

The work [29] also deserves attention, in which the Dubins car found an unexpected use for soft manipulators.

The constraint on the control does not necessarily have the form $u \in [-1, 1]$. A more general variant can be written as $u \in [u_1, u_2]$. For the case of $u_1 < 0$, $u_2 > 0$, synthesis of the time-optimal control is built in work [30]. Other models of motion are also studied; their description clearly comes from the Dubins car, but is more complex [10, Chapter 13], [31–34]. At the same time, the structure of the optimal controls often inherits the optimal structure of the similar problem with the dynamics of the Dubins car (see, e.g., work [35]).

The reachable set *at an instant* t_f under the given initial phase state at the instant t_0 is a set of all phase states, into each of which it is possible to transfer the system with the help of some permissible open-loop control exactly at the instant t_f. The reachable set at the instant t_f differs from the reachable set *up to the instant*. The latter consists of phase states, into each of which it is possible to transfer the system at some instant from the interval $[t_0, t_f]$.

For the numerical construction of the three-dimensional reachable sets, the grid methods (developed in the framework of the theory of differential games and Hamilton-Jacobi-Bellman partial differential equations) can be used. Examples of such constructions are given in works [36–39].

This paper examines the reachable set at an instant t_f. Let us denote it $G(t_f)$. For the constraint $u{\in}[-1, 1]$, an analytical description of boundary of the two-dimensional sections $G_\varphi(t_f)$ of the set $G(t_f)$ by the angular coordinate φ is given. In general, such φ-sections are non-convex and can be non-simply connected. Their structure depends on the instant t_f and the value φ. Description of the two-dimensional reachable set at an instant in geometric coordinates x, y (i.e., the projection of the three-dimensional set $G(t_f)$ into the plane x, y) was obtained in work [40]. Such set for any fixed t_f is the union of the sets $G_\varphi(t_f)$ over all possible φ under given t_f.

The results presented in this paper are based on the statements from paper [41] where (with the help of the Pontryagin maximum principle [42,43]) the statements about 6 types of piecewise constant open-loop control have been proven, by which one can limit when constructing the boundary of the set $G(t_f)$. In the main parts, the selected types in the main coincide with the variants obtained by L. Dubins in work [1].

Using these 6 types of the open-loop control, we analyze (with a fixed t_f) the ends of the corresponding motions that implement the specified value φ. Thus, in the φ-section of the set $G(t_f)$, a number of curves are selected, with the help of which the boundary of the φ-section is constructed. For $\varphi \geqslant 0$, we consider 5 different cases of the boundary formation of the φ-section. An analysis of some of these cases is very laborious.

The paper is organized as follows. In Section I, the problem statement is given. In Section II, information is given on 6 types of the extreme motions used to construct the boundary of the reachable set $G(t_f)$. For $\varphi \geqslant 0$, formulas for curves in φ-sections generated by extreme motions are derived. An auxiliary coordinate system is considered, which is more convenient than the original one when analyzing the properties of curves in the φ-sections. Curves are described, from the parts of which the boundary of φ-sections is constructed. The properties of these curves are analyzed. In particular, it is established that two curves represent parts of the involutes of the circle. Section III is devoted to statements about the extreme motions leading to the interior of the set $G(t_f)$. Auxiliary statements based on the Jordan curve theorem are given in Section IV. In Section V, classification of the φ-sections is given depending on the values t_f and φ. All possible variants are divided into five cases. In Sections VI–IX, the detailed analysis of each of these cases is given. Of particular interest is Case 2, for which the φ-sections are not simply connected. Section X describes the symmetry property that allows one to find the φ-sections for $\varphi < 0$ relying on the constructed φ-sections for $\varphi \geqslant 0$. Due to the limited size of the paper, proofs of some relations and auxiliary statements are omitted.

I Problem statement

Consider the controllable system

$$\dot{x} = \cos\varphi, \quad \dot{y} = \sin\varphi, \quad \dot{\varphi} = u; \quad u \in [-1, 1]. \tag{1}$$

Here, x and y are the coordinates of the geometric position in the plane, u is the scalar control. Let us agree that the positive value of the angle φ is counted from the positive direction of the axis x counterclockwise (Fig. 1). The phase vector $(x, y, \varphi)^{\mathsf{T}}$ of system (1) will be denoted by z.

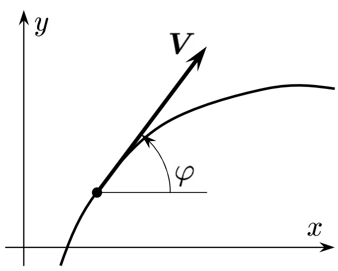

Fig. 1: The coordinate system, $\boldsymbol{V} = (\dot{x}, \dot{y})^{\mathsf{T}}$

As the initial state at the instant $t_0 = 0$, we set $x_0 = y_0 = \varphi_0 = 0$. The value of the angle φ at the instant t is calculated in the form of the integral

$$\int_0^t u(\tau)d\tau$$

of the open-loop control implemented on the interval $[0, t]$. Thus, $\varphi \in (-\infty, +\infty)$. As admissible open-loop controls, we take measurable functions of time that satisfy the constraint onto the control u.

The reachable set $G(t_f)$ is defined as the set of all those phase states of system (1) that can be obtained *at the instant* t_f using all the admissible measurable open-loop controls on the interval $[0, t_f]$. The choice of measurable controls as admissible is due to the desire to talk about the closedness of the reachable set $G(t_f)$ within the framework of the problem statement.

By the symbol $G_\varphi(t_f)$, we denote the φ-section of the set $G(t_f)$:

$$G_\varphi(t_f) = \{(x, y)^\top : (x, y, \varphi)^\top \in G(t_f)\}.$$

The purpose of this work is to obtain an analytical description of φ-sections.

The symbol ∂ will mean the boundary of the set, the symbol "int" is its interior. Note that if some point P belongs to $\partial G_\varphi(t_f)$, then the point $(P, \varphi)^\top$ belongs to $\partial G(t_f)$. Generally speaking, the reverse is not true.

II Properties of curves generated by extreme motions

II.A Types of extreme motions

Applying the Pontryagin maximum principle (PMP) to the open-loop controls transfering system (1) onto the boundary of the reachable set, we establish that for any point on the boundary there is some *piecewise constant* control leading to this point. The corresponding calculations are given in [41, 44]. It is shown that any point on the boundary of a three-dimensional set $G(t_f)$ can be reached using an open-loop control that takes values in a three-element set $\{-1, 0, 1\}$ and has no more than two switching instants. We identified 6 types of controls, by which one can limit to study of the boundary.

Let us list these 6 types. The switching instants are denoted by t_1 and t_2. We suppose that $t_f > 0$ and $0 = t_0 \leqslant t_1 \leqslant t_2 \leqslant t_f$.

A control of the type $U1$ takes the value $u = 1$ at some first time interval $[0, t_1)$, the value $u = 0$ is applied on some second interval $[t_1, t_2)$ and the value $u = 1$ is used on the third interval $[t_2, t_f]$. If one or two of the specified intervals are missing, then the resulting control is also assigned to the $U1$ type. The types $U2 - U6$ are defined similarly. Noting only the control values on each of three intervals, we shall write the corresponding table in the form

$$U1 : 1, 0, 1; \quad U2 : -1, 0, 1; \quad U3 : 1, 0, -1; \quad U4 : -1, 0, -1; \quad U5 : 1, -1, 1; \quad U6 : -1, 1, -1.$$

These types of controls coincide with those that were identified by L. Dubins in work [1] for solving the time-optimal problem. In relation to the controls of the types $U5$ and $U6$, additional conditions have been noted in the L. Dubins' work that are specific namely for the time-optimal problem. In the problem of constructing the boundary of the reachable set $G(t_f)$, the additional requirement for controls of the types $U5$ and $U6$ has the following form [41, p. 323]:

$$t_2 - t_1 \geqslant (t_1 - t_0) + (t_f - t_2). \tag{2}$$

In [41], it is shown that when inequality (2) is violated, the open-loop control of the type $U5$ or $U6$ leads to the interior of the reachable set $G(t_f)$.

Since the controls $U1 - U6$ satisfy the PMP, we call them and corresponding motions extreme. For the controls $U5$ and $U6$, we shall assume in the sequel that inequality (2) is fulfilled.

For each type of control, degeneration (reducing to zero) is possible of one or two intervals of control constancy. Formally, we shall refer such controls to more than one type of controls among $U1 - U6$.

The set of possible values φ of system (1) at the instant $t_f > 0$ is defined by the constraint $u \in [-1, 1]$ and represents the segment $[-t_f, t_f]$. The extreme values $\varphi = \mp t_f$ are provided on the controls $u(t) \equiv \mp 1$. We get the single-point φ-sections with the coordinates $x(t_f) = \sin t_f$, $y(t_f) = \mp(1 - \cos t_f)$.

For $\varphi > 0$, only 4 (namely, $U1$, $U2$, $U3$ and $U6$) from 6 types of control can lead to the boundary $\partial G_\varphi(t_f)$ of the corresponding φ-section. Indeed, control of the type $U4$ gives the value $\varphi \leqslant 0$ at the instant t_f. For control of the type $U5$ with $\varphi > 0$, condition (2) is violated.

Let $\varphi = 0$ at the instant t_f. Then the control of the type $U4$ is identically equal to zero and can also be assigned to the type $U1$. Now we take an arbitrary control of the type $U5$ with the switching instants t_1 and t_2. We have $t_0 \leqslant t_1 \leqslant t_2 \leqslant t_f$ and $t_2 - t_1 = (t_f - t_2) + (t_1 - t_0)$. Consider a control of the type $U6$ with the switches at the instants $t_1^* = t_f - t_2$ and $t_2^* = t_1^* + (t_2 - t_1)$. Integrating system (1), it is easy to verify that the designed control of the type $U6$ leads to the same point $(x(t_f), y(t_f))^\mathsf{T}$ as the initial control of the type $U5$. Therefore, for $\varphi = 0$, the controls of the type $U5$ generate the same set of points $(x, y)^\mathsf{T}$ at the instant t_f as the controls of the type $U6$.

Thus, the following lemma is valid.

Lemma 1. For $\varphi \in [0, t_f)$, to construct the boundary of φ-sections of the reachable set $G(t_f)$, we can restrict ourselves to four types of controls $U1$, $U2$, $U3$, and $U6$.

Further, when studying the φ-sections, detailed calculations are made under the assumption $0 \leqslant \varphi < t_f$. The constructed φ-sections taking into account the symmetry of system (1) determine φ-sections for the condition $-t_f < \varphi < 0$ using some linear transformation.

II.B Formulas in the original coordinates for curves in φ-sections

Fixing a certain value of φ at the instant $t_f > 0$, we get a connection between the switching instants t_1 and t_2, which provides this φ. Thus, for each control type providing the selected φ, we get corresponding one-parameter curve in the plane x, y.

We assume that $\varphi \geqslant 0$. In accordance with Lemma 1, we use controls of the types $U1$, $U2$, $U3$, and $U6$ to construct the boundary of the φ-sections.

Introduce the notation $\theta = (t_f - \varphi)/2$. Obviously, for $\varphi \in [0, t_f)$, the inequalities $\theta > 0$, $\theta + \varphi > 0$ are fulfilled.

We give formulas describing the geometric positions in the plane x, y by virtue of controls of the types $U1$, $U2$, $U3$, and $U6$ for the selected values t_f and φ. The corresponding one-dimensional parameters s_1, s_2, s_3, and s_6 are determined using the formulas

$$s_1 = 2t_1 - \varphi, \quad s_2 = -t_1, \quad s_3 = t_1 - \varphi, \quad s_6 = 2t_1 - \theta. \tag{3}$$

We shall take the ranges of acceptable values of these parameters in the form

$$\begin{aligned} s_1 &\in \left[s_1^b, s_1^e\right] = [\,-\varphi,\, \varphi\,], \quad & s_2 &\in \left[s_2^b, s_2^e\right] = [\,-\theta,\, 0\,], \\ s_3 &\in \left[s_3^b, s_3^e\right] = [\,0,\, \theta\,], \quad & s_6 &\in \left[s_6^b, s_6^e\right] = [\,-\theta,\, \theta\,]. \end{aligned} \tag{4}$$

Integrating system (1) for four types of the controls under consideration, we get

$$\begin{pmatrix} x_{U1}(s_1) \\ y_{U1}(s_1) \end{pmatrix} = \begin{pmatrix} \sin\varphi \\ 1-\cos\varphi \end{pmatrix} + (t_f-\varphi)\begin{pmatrix} \cos\left(\dfrac{s_1+\varphi}{2}\right) \\ \sin\left(\dfrac{s_1+\varphi}{2}\right) \end{pmatrix}, \tag{5}$$

$$\begin{pmatrix} x_{U2}(s_2) \\ y_{U2}(s_2) \end{pmatrix} = \begin{pmatrix} \sin\varphi \\ 1-\cos\varphi \end{pmatrix} + 2\left((\theta+s_2)\begin{pmatrix} \cos s_2 \\ \sin s_2 \end{pmatrix} - \begin{pmatrix} \sin s_2 \\ 1-\cos s_2 \end{pmatrix}\right), \tag{6}$$

$$\begin{pmatrix} x_{U3}(s_3) \\ y_{U3}(s_3) \end{pmatrix} = -\begin{pmatrix} \sin\varphi \\ 1-\cos\varphi \end{pmatrix} + 2\left((\theta-s_3)\begin{pmatrix} \cos(s_3+\varphi) \\ \sin(s_3+\varphi) \end{pmatrix} + \begin{pmatrix} \sin(s_3+\varphi) \\ 1-\cos(s_3+\varphi) \end{pmatrix}\right), \tag{7}$$

$$\begin{pmatrix} x_{U6}(s_6) \\ y_{U6}(s_6) \end{pmatrix} = -\begin{pmatrix} \sin\varphi \\ 1-\cos\varphi \end{pmatrix} + 4\sin\left(\frac{t_f+\varphi}{4}\right)\begin{pmatrix} \cos\left(\dfrac{\varphi-s_6}{2}\right) \\ \sin\left(\dfrac{\varphi-s_6}{2}\right) \end{pmatrix}. \tag{8}$$

In work [45], the case $t_f \leqslant 2\pi$ was considered. There, other (but equivalent) formulas for the parametric description of these curves in the original coordinate system x, y were obtained. The relations presented above are more compact.

II.C Auxiliary coordinate system

We shall use an auxiliary orthogonal coordinate system as in work [45]. It is convenient for revealing the symmetry properties of the φ-sections boundary. We define the auxiliary system X, Y through the original system x, y as follows:

$$\begin{pmatrix} X \\ Y \end{pmatrix} = \begin{pmatrix} \cos(\varphi/2) & \sin(\varphi/2) \\ -\sin(\varphi/2) & \cos(\varphi/2) \end{pmatrix}\left(\begin{pmatrix} x \\ y \end{pmatrix} - \begin{pmatrix} \sin\varphi \\ 1-\cos\varphi \end{pmatrix}\right). \tag{9}$$

For a fixed φ, this linear transformation consists of a rotation and a shift. It is one-to-one and preserves the distance between points.

The axis X of the auxiliary system passes through the origin of the initial system (point o) and is rotated by an angle $\varphi/2$ counterclockwise relative to the axis x (Fig. 2). The reference point of the auxiliary system (point O) coincides with the center of the circumference containing the arc (5). The axis X divides this arc in half.

We denote by A1, A2, A3, and A6 curves (5), (6), (7), and (8), which are generated by the controls $U1$, $U2$, $U3$, and $U6$ in the auxiliary system. Their analytical representation has the form

$$\mathrm{A1}(s_1) = \begin{pmatrix} X_{U1}(s_1) \\ Y_{U1}(s_1) \end{pmatrix} = (t_f-\varphi)\begin{pmatrix} \cos\left(\frac{s_1}{2}\right) \\ \sin\left(\frac{s_1}{2}\right) \end{pmatrix} = 2\theta\begin{pmatrix} \cos\left(\frac{s_1}{2}\right) \\ \sin\left(\frac{s_1}{2}\right) \end{pmatrix}, \tag{10}$$

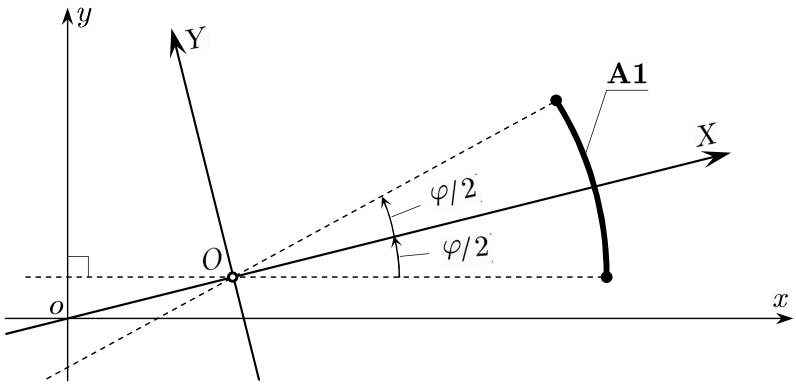

Fig. 2: Auxiliary coordinate system X, Y

$$\mathrm{A2}(s_2) = \begin{pmatrix} X_{U2}(s_2) \\ Y_{U2}(s_2) \end{pmatrix} = 2\,(\theta + s_2) \begin{pmatrix} \cos\left(s_2 - \dfrac{\varphi}{2}\right) \\ \sin\left(s_2 - \dfrac{\varphi}{2}\right) \end{pmatrix} - 4\sin\left(\frac{s_2}{2}\right) \begin{pmatrix} \cos\left(\dfrac{s_2}{2} - \dfrac{\varphi}{2}\right) \\ \sin\left(\dfrac{s_2}{2} - \dfrac{\varphi}{2}\right) \end{pmatrix}, \quad (11)$$

$$\mathrm{A3}(s_3) = \begin{pmatrix} X_{U3}(s_3) \\ Y_{U3}(s_3) \end{pmatrix} = 2\,(\theta - s_3) \begin{pmatrix} \cos\left(s_3 + \dfrac{\varphi}{2}\right) \\ \sin\left(s_3 + \dfrac{\varphi}{2}\right) \end{pmatrix} + 4\sin\left(\frac{s_3}{2}\right) \begin{pmatrix} \cos\left(\dfrac{s_3}{2} + \dfrac{\varphi}{2}\right) \\ \sin\left(\dfrac{s_3}{2} + \dfrac{\varphi}{2}\right) \end{pmatrix}, \quad (12)$$

$$\mathrm{A6}(s_6) = \begin{pmatrix} X_{U6}(s_6) \\ Y_{U6}(s_6) \end{pmatrix} = -4 \begin{pmatrix} \sin\left(\dfrac{\varphi}{2}\right) \\ 0 \end{pmatrix} + 4\sin\left(\frac{t_f + \varphi}{4}\right) \begin{pmatrix} \cos\left(\dfrac{-s_6}{2}\right) \\ \sin\left(\dfrac{-s_6}{2}\right) \end{pmatrix}. \quad (13)$$

The parameters s_1, s_2, s_3, s_6 and the corresponding ranges of their changes are defined in (3), (4).

Further analysis of the φ-sections of the reachable set $G(t_f)$ will be carried out in the auxiliary coordinate system.

II.D The simplest properties of curves A1, A2, A3, and A6

The curves A1 and A6 are arcs of circumferences. Each of them is symmetric w.r.t. the axis X, since the following relations are valid:

$$X_{A1}(s_1) = X_{A1}(-s_1), \qquad Y_{A1}(s_1) = -Y_{A1}(-s_1);$$

$$X_{A6}(s_6) = X_{A6}(-s_6), \qquad Y_{A6}(s_6) = -Y_{A6}(-s_6).$$

The center of the circumference, the arc of which is the curve A1, coincides with the origin of the auxiliary system. The radius R_{A1} of the circumference is calculated using the formula

$$R_{A1} = 2\theta = t_f - \varphi. \quad (14)$$

The angular span of the arc A1 is equal to φ. Therefore, the curve A1 has no self-intersections for $\varphi \in [0, 2\pi)$. For $\varphi \geqslant 2\pi$, the curve A1 covers the entire circumference.

The "overlap" points can be reached at different values of the parameter s_1, which differ by 4π. If $\varphi = 0$, then the curve A1 degenerates to the point $(t_f, 0)^{\mathsf{T}}$. Let us denote by the symbol C_{A1} the circle of the radius R_{A1} with the center at the origin of the auxiliary coordinate system.

The center of the circumference, the arc of which is the curve A6, is located at the point

$$H = -4\,(\sin(\varphi/2),\, 0)^{\mathsf{T}}\,, \tag{15}$$

on the axis X. The radius R_{A6} of the circumference is equal to

$$R_{A6} = 4\,|\sin((t_f + \varphi)/4)|\,. \tag{16}$$

Its value depends on t_f, φ and becomes zero when $(t_f + \varphi)$ is multiple of 4π. The angular span of the arc A6 is equal to θ. If $(t_f + \varphi) < 4\pi$, then $\theta < 2\pi$ and the curve A6 has no self-intersections. We denote by the symbol C_{A6} the circle of the radius R_{A6} with the center at the point H.

The curves A2 and A3 are mutually symmetric w.r.t. the axis X. This property is defined by equalities

$$X_{A2}(s_2) = X_{A3}(s_3), \qquad Y_{A2}(s_2) = -Y_{A3}(s_3), \tag{17}$$

that are valid for any parameter values $s_2 = -s_3$ from ranges (4).

For controls of the type $U3$ forming the curve A3, let us analyze the degeneracy of the control constancy intervals. The first interval is non-degenerate for $s_3 > 0$, since we have $t_1 = \varphi + s_3 > 0$ by virtue of (3) and (4). Duration of the second interval is determined by the formula $t_2 - t_1 = t_f - \varphi - 2s_3$. It vanishes only when $s_3 = (t_1 - \varphi)/2 = \theta$, i.e., at the last point of the curve A3. Duration of the third interval is $t_f - t_2 = s_3$. Therefore, the third interval degenerates only at the initial point of the curve A3. Thus, none of the control constancy intervals degenerates for the internal points of the curve A3. The similar property is true for the curve A2.

In Fig. 3, the curve A3 corresponding to $\varphi = 0.3\pi$ and $t_f = 2.7\pi$ is shown. The geometric method of constructing points A3(s_3) by controls of the type $U3$ is explained for several values of the parameter s_3. The motions leave the starting point o with the direction indicated by the arrow. On the interval $[0, t_1)$, each motion goes with $u = +1$ along the dotted circumference counterclockwise. Then, it continues on the interval $[t_1, t_2)$ by a straight-line motion with $u = 0$. The third interval $[t_2, t_f]$ corresponds to the motion along the arc of the circumference with $u = -1$ clockwise.

Consider the curves A1, A2, A3, and A6 in the sequence A1, A3, A6, and A2 bypassing them in ascending parameters s_1, s_2, s_3, and s_6. For the extreme values of the parameters, we have

$$\mathrm{A1}(s_1^e) = \mathrm{A3}(s_3^b), \quad \mathrm{A3}(s_3^e) = \mathrm{A6}(s_6^b), \quad \mathrm{A6}(s_6^e) = \mathrm{A2}(s_2^b), \quad \mathrm{A2}(s_2^e) = \mathrm{A1}(s_1^b).$$

The listed docking points are denoted by $\mathcal{P}_{1,3}$, $\mathcal{P}_{3,6}$, $\mathcal{P}_{2,6}$, and $\mathcal{P}_{1,2}$. As a result of splicing, we get a continuous piecewise smooth closed curve, which we denote by the symbol $\mathrm{A}_\varphi(t_f)$.

By virtue of Lemma 1, the boundary of the φ-section for $\varphi \in [0, t_f)$ is a subset of the curve $\mathrm{A}_\varphi(t_f)$. When selecting parts of the curves A1, A3, A6, and A2 that form the boundary of the φ-section, significant difficulty is caused by the presence of self-intersections of the curve $\mathrm{A}_\varphi(t_f)$.

In Fig. 4, two examples of the curve $\mathrm{A}_\varphi(t_f)$ are given. The docking points of the curves A1, A3, A6, and A2 are marked with risks. For the values $t_f = 3\pi$ and $\varphi = 0.4\pi$ (Fig. 4a),

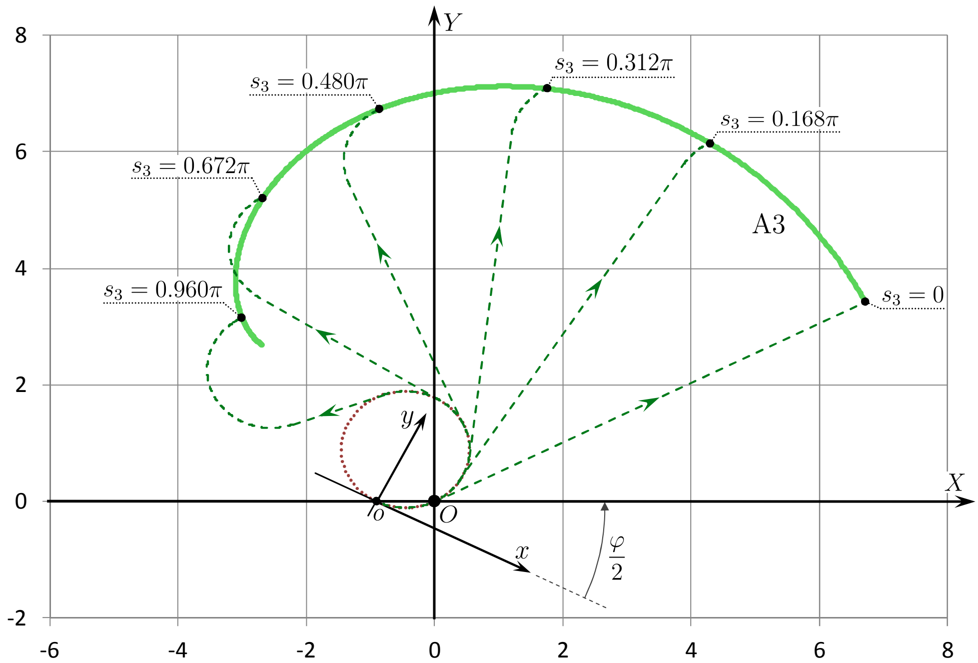

Fig. 3: Formation of the curve A3 by means of controls of the type $U3$

the curve $\mathrm{A}_\varphi(t_f)$ has no self-intersections. There are many self-intersection points for the values $t_f = 10\pi$ and $\varphi = 0.4\pi$ (Fig. 4b). When changing s_6 in the range $[-\theta; \theta]$, points $\mathrm{A6}(s_6)$ go along the boundary of the circle C_{A6} clockwise from the point of docking with the curve A3 to the point of docking with the curve A2. Herewith, on Fig. 4b, the point $\mathrm{A6}(s_6)$ makes more than two turns.

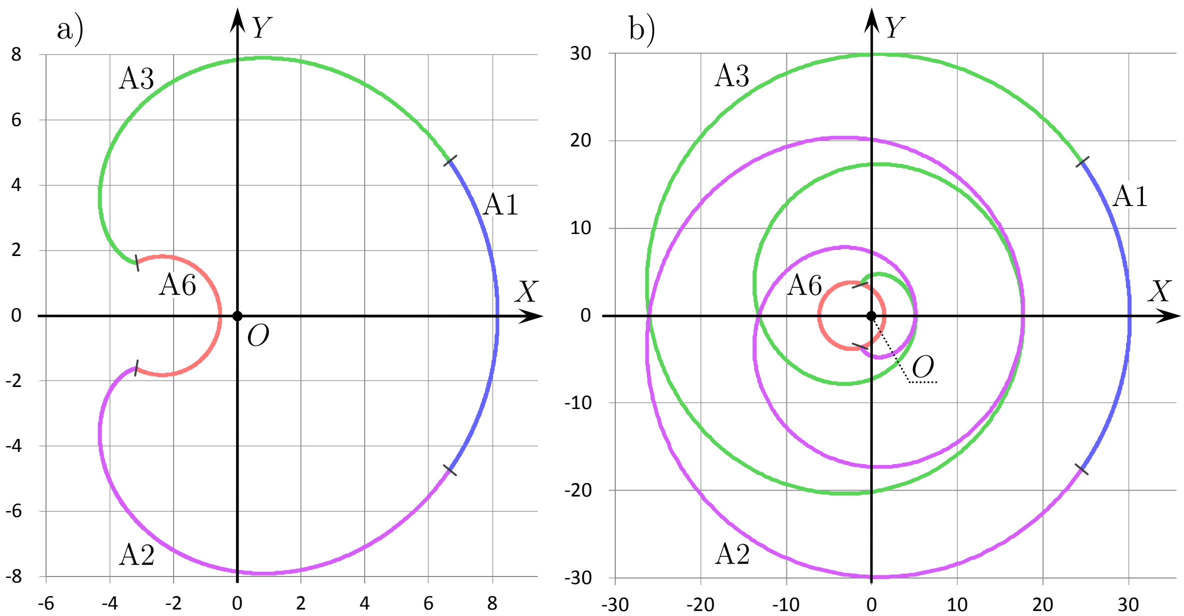

Fig. 4: The curve $\mathrm{A}_\varphi(t_f)$ for $t_f = 3\pi$, $\varphi = 0.4\pi$ (a) and $t_f = 10\pi$, $\varphi = 0.4\pi$ (b)

Structure of the curve $\mathrm{A}_\varphi(t_f)$ (for a fixed φ) becomes more complicated with the growth of t_f.

Further in this section, location of the curves A1, A2, A3, and A6 in the plane X, Y will be investigated.

II.E Curves A2 and A3 are parts of circle involutes

Each of the curves A2 and A3 is some part of the involute of the circle. We show it for the curve A2. Let us rewrite equation (11) for the curve A2 in equivalent form, using the trigonometric transformation of the last term:

$$\mathrm{A2}(s_2) = 2\,(\theta + s_2)\begin{pmatrix} \cos\left(s_2 - \dfrac{\varphi}{2}\right) \\ \sin\left(s_2 - \dfrac{\varphi}{2}\right) \end{pmatrix} + 2\begin{pmatrix} -\sin\left(s_2 - \dfrac{\varphi}{2}\right) \\ \cos\left(s_2 - \dfrac{\varphi}{2}\right) \end{pmatrix} - 2\begin{pmatrix} \sin\left(\dfrac{\varphi}{2}\right) \\ \cos\left(\dfrac{\varphi}{2}\right) \end{pmatrix}. \tag{18}$$

The canonical form of the parametric representation of the involute of a circle is taken in the following form (see [46, p. 252, formula (1)], [47, §11, p. 43]):

$$\begin{aligned} x_1 &= r\cos\tau + r\tau\sin\tau, \\ x_2 &= r\sin\tau - r\tau\cos\tau. \end{aligned} \tag{19}$$

Here, x_1 and x_2 are the rectangular coordinates, $\tau \geqslant 0$ is a parameter. The radius of the base circle is r, its center is located at the origin. The involute at $\tau = 0$ leaves the point $(0,\, r)^{\mathsf{T}}$.

Let us represent the curve A2, given by formula (18), in form (19) using the rotation and shift operations. The shift is provided by the third term in (18), it does not depend on s_2. Next, we shall replace the variables $\tau = \theta + s_2, \tau \in [0,\, \theta]$. After that, the first two terms in (18) (after rearranging them) will be written as follows:

$$2\begin{pmatrix} -\sin\left(\tau - \theta - \dfrac{\varphi}{2}\right) \\ \cos\left(\tau - \theta - \dfrac{\varphi}{2}\right) \end{pmatrix} + 2\tau\begin{pmatrix} \cos\left(\tau - \theta - \dfrac{\varphi}{2}\right) \\ \sin\left(\tau - \theta - \dfrac{\varphi}{2}\right) \end{pmatrix}. \tag{20}$$

Further, we introduce the rotation matrix

$$\begin{pmatrix} \cos\psi & \sin\psi \\ -\sin\psi & \cos\psi \end{pmatrix}$$

and multiply it by vector (20). Assuming $\psi = \dfrac{\pi}{2} - \theta - \dfrac{\varphi}{2}$, we get for (20) representation of form (19):

$$2\begin{pmatrix} \cos\tau \\ \sin\tau \end{pmatrix} + 2\tau\begin{pmatrix} \sin\tau \\ -\cos\tau \end{pmatrix}.$$

Thus, the curve A2 is the initial part of the involute of the circle. As a result, it does not have self-intersections. The center of the base circle is located at the point $2\,(\,-\sin(\varphi/2),\; -\cos(\varphi/2)\,)^{\mathsf{T}}$, its radius is 2. The starting point of the involute corresponds to the value $s_2 = -\theta$.

The curve A3 is symmetric to the curve A2 and, also, represents the initial part of the involute of the circle. For it, the radius of the base circle is the same as for the curve A2, and its center is located at the point $2\,(\,-\sin(\varphi/2),\; \cos(\varphi/2)\,)^{\mathsf{T}}$ symmetrically w.r.t. the axis X.

Note that the point O of the auxiliary system X, Y origin always belongs to both base circles.

In Fig. 5 for $t_f = 2.5\pi$ and $\varphi = \pi/3$, the base circles corresponding to the involutes A3 and A2 are shown. Dotted straight lines generate points of the curve A3 (respectively, of the curve A2) as the points of the circle's involute. Curves A1 and A6 are also presented.

We emphasize that the dotted lines (coming to the curve A3 or the curve A2) are not the trajectories of the system (1) from the initial phase point $x_0 = y_0 = \varphi_0 = 0$ and do not satisfy the boundary condition for φ when hitting the curve A3 or the curve A2.

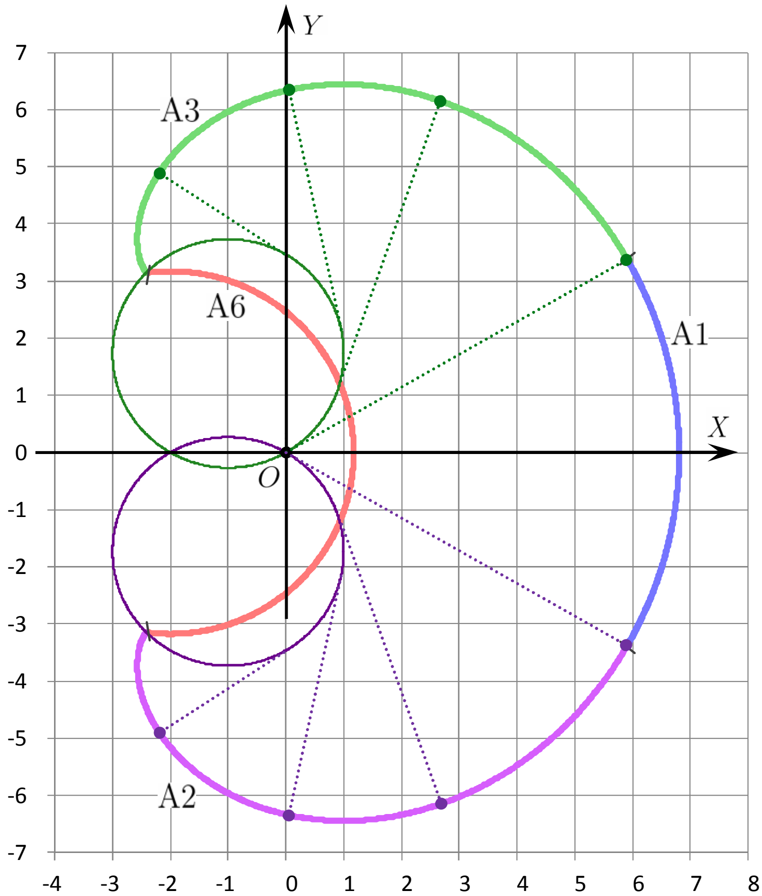

Fig. 5: Representation of the curves A3 and A2 in the form of involutes

II.F Mutual arrangement of curves A1, A2, A3, and A6

Denote by the symbol $R_{1,6}(s_6)$ the distance from the center of the curve A1 (it coincides with the origin O of the auxiliary system) to the points of the curve A6. Let $R_{6,1}(s_1)$, $R_{6,2}(s_2)$, and $R_{6,3}(s_3)$ be respectively distances from the center H of the curve A6 to the points of the curves A1, A2, and A3.

The denotations used here are illustrated in Fig. 6. Calculations are made for $t_f = 2.4\pi$ and $\varphi = 0.8\pi$.

1) Let us start with the analysis of the relative arrangement of the curves A1 and A6. The corresponding relation is valid (it is not trivial, the proof is omitted):

$$(R_{A1})^2 - (R_{1,6}(s_6))^2 > 0, \qquad s_6 \in \left[s_6^b, s_6^e\right] = [-\theta, \theta]. \tag{21}$$

It follows from this relation that the curve A6 belongs to $\mathrm{int}C_{A1}$. Therefore, the arcs A1 and A6 do not have common points.

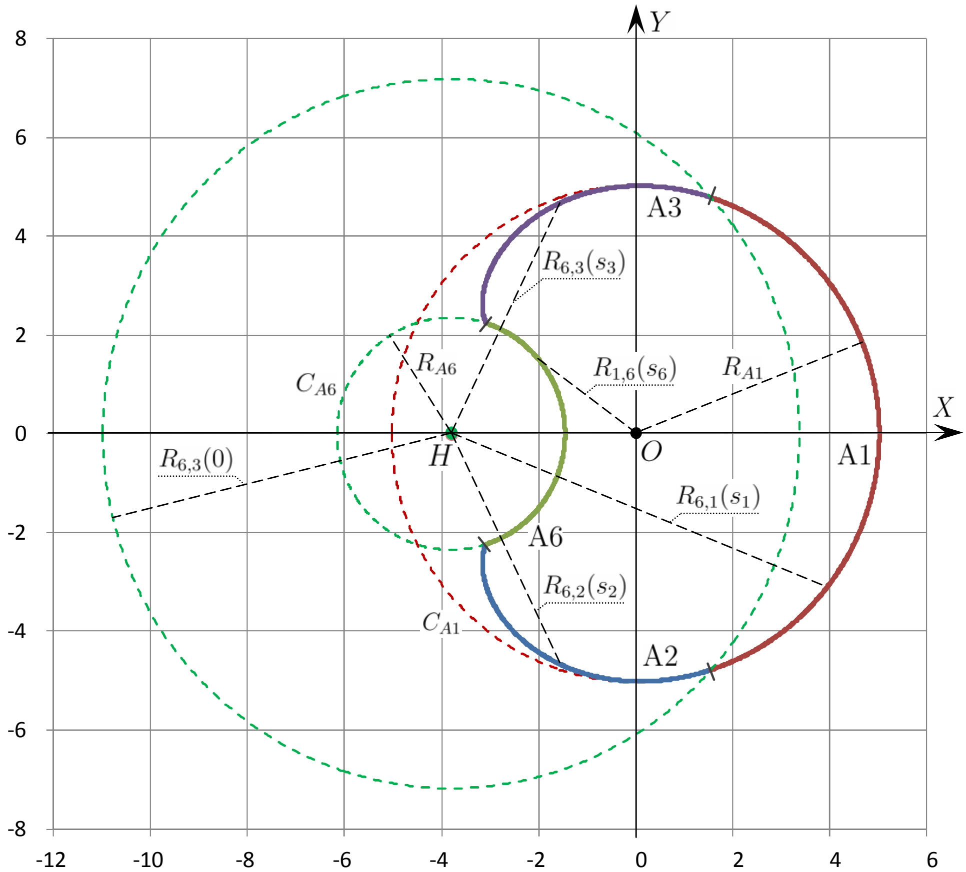

Fig. 6: Explanation of denotations for the study of the mutual arrangement of the curves A1, A2, A3, and A6

2) Let describe the docking of the curves A2 and A3 with the curve A1.

The radius of curvature of the involute at the current point is the distance from it along the generating straight line to the contact point of the line with the base circle [46, p. 252].

For the involute A3 at the current value of the parameter s_3, the point of contact of the generating straight line with the base circle is a vector representing the second term in the right part of formula (12). The radius of curvature of the curve A3 at the current point is the modulus of the first term in (12), *i.e.*, $2\,(\theta - s_3)$. For the starting point of the curve A3 (where $s_3 = 0$), the point of tangency of the generating straight line with the base circle coincides with the origin of the coordinates of the plane X, Y, and the radius of curvature is 2θ. The circumpherence, on which the arc A1 lies, has the same center and the same radius. Consequently, the curves A1 and A3 are smoothly joined with the coincidence of curvature. Since the radius of curvature of the involute A3 monotonically decreases with the growth of s_3, then the entire curve A3 (excepting the starting point) belongs to intC_{A1} [48, Theorem 2]. It follows that the curves A1 and A3 have only one common point (i.e., the junction point $\mathcal{P}_{1,3}$).

Similarly, due to symmetry, the curve A2 (excepting the point $\mathcal{P}_{1,2}$ that is the point of junction with the curve A1) belongs to intC_{A1}.

3) To estimate the relative location of the curves A2 and A6, consider the function $s_2 \rightarrow (R_{6,2}(s_2))^2$. Based on (11) and (13), we can show that the function $(R_{6,2}(s_2))^2$ is strictly monotonically increasing w.r.t. the parameter s_2. Therefore, for $\varphi < t_f$, the inequality $R_{6,2}(s_2) > R_{A6}$ is valid for all $s_2 \in \left(s_2^b, s_2^e\right]$. The similar inequality $R_{6,3}(s_3) > R_{A6}$ is also fulfilled for the points of the curve A3.

4) Let $0 \leqslant \varphi < 2\pi$. Analyzing the difference

$$(R_{6,1}(s_1))^2 - (R_{6,3}(0))^2 \,,$$

one can establish that the curve A1 lies outside the interior of the circle with the center at the point H and the radius equal to the distance from the point H to the points $\mathcal{P}_{1,3}$ and $\mathcal{P}_{1,2}$. The minimum distance from the point H to the points of the curve A1 is acheived at the points $\mathcal{P}_{1,3}$ and $\mathcal{P}_{1,2}$, i.e., $R_{6,1}(-\varphi) = R_{6,1}(\varphi) \leqslant R_{6,1}(s_1)$ for any $s_1 \in [-\varphi, \varphi]$.

5) Let us prove that the curves A2 and A3 can intersect only at points on the axis X.

Suppose the opposite that outside the axis X, there is a point of intersection of the curves A2 and A3, and it corresponds to some values of the parameters $\widetilde{s}_2$ and $\widetilde{s}_3$. The curves A2 and A3 are symmetric w.r.t. the axis X. Therefore, there is a point on the curve A3 corresponding to some parameter $\widehat{s}_3$, for which $X_{U3}(\widehat{s}_3) = X_{U2}(\widetilde{s}_2)$, $Y_{U3}(\widehat{s}_3) = -Y_{U2}(\widetilde{s}_2)$. Since $Y_{U3}(\widehat{s}_3) = -Y_{U3}(\widetilde{s}_3) \neq 0$, then $\widehat{s}_3 \neq \widetilde{s}_3$. Thus, two different points were obtained on the curve A3, symmetric w.r.t. the axis X. Therefore, they are equally distanced from any point on the axis X, in particular, from the point H. Above, the strict monotony of changing the distance from the point H to the points of the curve A3 was established. Therefore, the points of the curve A3 specified by the parameters $\widetilde{s}_3$ and $\widehat{s}_3$ have different distances to the point H. We came to the contradiction.

II.G List of properties of curves A1, A2, A3, and A6

Let us summarize the properties of the curves A1, A2, A3, and A6 in the plane X, Y at $0 \leqslant \varphi < t_f$.

1. Each of the curves A1 and A6 is symmetric w.r.t. the axis X and is an arc of the circumference, whose center lies on the axis X. The span of the arc can be greater than 2π. The curve A1 degenerates to a point only when $\varphi = 0$. The curve A6 degenerates to a point only when $(t_f + \varphi)$ is multiple to 4π.

2. Each of the curves A2 and A3 represents the initial part of the involute of the circle, therefore, it does not have self-intersections.

3. The curves A2 and A3 are mutually symmetric w.r.t. the axis X and can intersect only at points on this axis.

4. All internal points of the curve A2 (respectively, A3) are generated by controls of the type $U2$ ($U3$) with three non-degenerate constancy intervals.

5. The distance $R_{6,2}(s_2)$ from the center H of the circle C_{A6} to the point on the curve A2 (defined by the parameter s_2) increases monotonically as the parameter s_2 grows.

6. The distance $R_{6,3}(s_3)$ from the center H of the circle C_{A6} to the point on the curve A3 (defined by the parameter s_3) decreases monotonically as the parameter s_3 grows.

7. The curves A2 and A3 are smoothly mated with the curve A1. The radii of curvature at the docking points are the same.

8. The curves A2 and A3 (excepting the points of their junction with the curve A1), as well as, the entire curve A6 lie in the interior of the circle C_{A1}.

9. The curves A2 and A3 (excepting the points of their junction with the curve A6) lie outside the circle C_{A6}.

10. For $\varphi \in [0, 2\pi)$, the distance from the center H of the circle C_{A6} to the curve A1 is acheived at the curve extreme points.

11. Connection of the curves A1, A2, A3, and A6 forms a piecewise smooth closed curve that is symmetric w.r.t. the axis X.

III Auxiliary statements about extreme motions leading to the interior of the reachable set $G(t_f)$

Paper [41] contained statements characterizing the extreme motions leading to the interior of the reachable set $G(t_f)$. In this paper, additional statements on this topic will be required.

When considering them, we shall use the following property [41, 44]. Let some control $u^*(\cdot)$ and the corresponding motion $z^*(\cdot)$ of system (1) satisfy the PMP. Then, if the control $u^*(\cdot)$ has more than two switching instants, then the geometric positions of $(x^*(t), y^*(t))^{\mathsf{T}}$ at these instants lie on a single straight line, which is called the switching one. Also, if the control $u^*(\cdot)$ has an interval with $u^*(t) \equiv 0$, then the corresponding part of the rectilinear motion in the plane x, y lies on the straight switching line.

Now we give two statements about extreme motions with cycles. By a cycle, we mean a part of motion with the constant control $u = \pm 1$ and the length greater or equal to 2π.

Lemma 2. Let the motion $z(\cdot)$ of system (1) be generated by a control of the type $U2$ or $U3$ with three non-degenerate control constancy intervals. If at least one of the two extreme intervals has duration of at least 2π, then $z(t_f) \in \mathrm{int}G(t_f)$.

Lemma 3. Let the motion $z(\cdot)$ of system (1) be generated by a control of the type $U6$. Wherein, some two adjacent intervals of the control constancy are non-degenerate. If at least one of them has duration greater than 2π, then $z(t_f) \in \mathrm{int}G(t_f)$.

The following Lemma is fundamental. But its proof is very long and is also omitted.

Lemma 4. Let the motion $z(\cdot)$ be generated by a control of the type $U3$ and lead to the point $z(t_f) = (x(t_f), y(t_f), \varphi(t_f))^{\mathsf{T}}$, for which $\varphi(t_f) \geqslant 0$. Suppose that for the point $(x(t_f), y(t_f))^{\mathsf{T}}$ after transferring it to the auxiliary system X, Y, the inequality $Y(t_f) < 0$ is fulfilled. In addition, we assume that all three sections of constancy of the control are non-degenerate, and the duration of both the first and third intervals is less than 2π. Then $z(t_f) \in \mathrm{int}G(t_f)$.

IV Statements about the structure of φ-sections

Proofs of Lemmas 5 and 6 formulated below are based on the Jordan curve theorem [49, 50], which characterizes partition of the plane by a continuous closed curve S without self-intersections. According to the Jordan theorem, the set $\mathbb{R}^2 \backslash S$ consists of two open, connected and disjoint components S^+ (external unlimited) and S^- (internal limited). The curve S is the boundary of these components.

Lemmas 5 and 6 are used later to construct the boundary of φ-sections. Lemma 7 will also be used in the sequel.

Lemma 5. Consider some values $t_f > 0$ and $\varphi \in [0, t_f)$. Let S be a continuous closed curve without self-intersections in the plane x, y, to any point of which at the instant t_f (with a given value φ), at least one of the controls of the types $U1$, $U2$, $U3$, and $U6$ leads. Suppose that in S^+ there are no points formed by controls of the types $U1$, $U2$, $U3$, and $U6$ for the mentioned values t_f and φ. Then $S \subset \partial G_\varphi(t_f)$. Herewith, $G_\varphi(t_f) \cap S^+ = \varnothing$.

Lemma 6. Consider some values $t_f > 0$ and $\varphi \in [0, t_f)$. Let S be a continuous closed curve without self-intersections in the plane x, y, to any point of which at the instant t_f (with a given value φ), at least one of the controls of the types $U1$, $U2$, $U3$, and $U6$ leads. Suppose that in S^-, there are no points formed by controls of the types

$U1$, $U2$, $U3$, and $U6$ for the mentioned values t_f and φ. Also, assume that in S^-, there is at least one point that does not belong to the set $G_\varphi(t_f)$. Then $S \subset \partial G_\varphi(t_f)$. Herewith, $G_\varphi(t_f) \cap S^- = \varnothing$.

Lemma 7. Consider some values $t_f > 0$ and $\varphi \in [0,\, t_f)$. Let a set M in the plane of geometric coordinates x, y be open and connected. Assume that one of the following conditions is valid: 1) there are no points of curves A1, A2, A3, and A6 in the set M, but there is at least one point $P \in \mathrm{int} G_\varphi(t_f)$; 2) in the set M, there are points of some curves A1, A2, A3, and A6, but any such point belongs to $\mathrm{int} G_\varphi(t_f)$ excepting, perhaps, only one point. Then $M \subset \mathrm{int} G_\varphi(t_f)$.

V Classification of φ-sections for $\varphi \geqslant 0$

The shape of the φ-sections is determined by the values of φ and t_f. Assume that $t_f > 0$ and $\varphi \in [0,\, t_f]$. We shall distinguish five sets in the space of values φ, t_f. Respectively, we consider five cases

$$\text{Case 1:} \quad 0 \leqslant \varphi < t_f, \quad t_f < 4\pi - \varphi, \quad t_f < 3\pi + 2\cos(\varphi/2). \tag{22}$$

$$\text{Case 2:} \quad 0 \leqslant \varphi < \pi, \quad t_f < 4\pi - \varphi, \quad t_f \geqslant 3\pi + 2\cos(\varphi/2). \tag{23}$$

$$\text{Case 3:} \quad 0 \leqslant \varphi < 2\pi, \quad t_f \geqslant 4\pi - \varphi. \tag{24}$$

$$\text{Case 4:} \quad 2\pi \leqslant \varphi < t_f. \tag{25}$$

$$\text{Case 5:} \quad \varphi = t_f. \tag{26}$$

Let us establish that any point $(\varphi,\, t_f)$ satisfying the conditions $t_f > 0$ and $0 \leqslant \varphi \leqslant t_f$ belongs to one and only one of the specified sets.

If $\varphi = t_f$, then we deal with Set 5 (Case 5). With that, it is obvious that the point $(\varphi,\, t_f)$ does not come into Set 1 and Set 4. In Case 2, it follows from the first and third conditions (23) that $t_f > 3\pi$. In Case 3, we have $t_f > 2\pi$. Thus, the point under consideration does not belong to Sets $1-4$.

From the first two inequalities in (22), it follows that in Case 1 the inequality $\varphi < 2\pi$ holds. Therefore, under condition (25), the point $(\varphi,\, t_f)$ comes only into Set 4.

If $0 \leqslant \varphi < \pi$, then the inequality

$$4\pi - \varphi > 3\pi + 2\cos(\varphi/2) \tag{27}$$

holds. Indeed, the condition $0 \leqslant \varphi < \pi$ can be rewritten as $0 < (\pi - \varphi)/2 \leqslant \pi/2$. Therefore, the inequality $(\pi - \varphi)/2 > \sin((\pi - \varphi)/2)$ holds that is equivalent to (27). Inequality (27) means that for $0 \leqslant \varphi < \pi$ in (22), the second condition follows from the third condition. Similarly, for $\varphi \in [\pi, 2\pi)$, we have

$$4\pi - \varphi \leqslant 3\pi + 2\cos(\varphi/2), \tag{28}$$

i.e., in (22), the third condition follows from the second one.

Let $0 \leqslant \varphi < \pi$ and $\varphi < t_f$. Based on inequality (27), we establish that the point (φ, t_f) comes at $t_f \in (\varphi, 3\pi + 2\cos(\varphi/2))$ only to Set 1; correspondingly, for $t_f \in [3\pi + 2\cos(\varphi/2), 4\pi - \varphi)$ only to Set 2 and only to Set 3 for $t_f \in [4\pi - \varphi, \infty)$. Let $\varphi \in [\pi, 2\pi)$ and $\varphi < t_f$. Using inequality (28), we get that the point (φ, t_f) belongs only to Set 1 for $t_f < 4\pi - \varphi$ and only to Set 3 for $t_f \geqslant 4\pi - \varphi$.

Thus, the property of partition of the area $\{(\varphi,\, t_f) : 0 \leqslant \varphi \leqslant t_f,\, t_f > 0\}$ into Sets $1-5$ is established.

Sets $1-5$ are shown in Fig. 7. For $0 \leqslant \varphi < \pi$, Set 1 is separated from Set 2 by the line $t_f = 3\pi + 2\cos(\varphi/2)$ (the line is included into Set 2), and Set 2 is separated from Set 3 by a segment of the straight line $t_f = 4\pi - \varphi$ (that is included into Set 3). For $\pi \leqslant \varphi < 2\pi$, Set 1 is separated from Set 3 by a segment of the straight line $t_f = 4\pi - \varphi$; this segment is included into Set 3. Set 3 is separated from Set 4 by an unlimited ray $\varphi = 2\pi, t_f > \varphi$, which is included into Set 4. Set 5 is an unlimited ray $0 < \varphi = t_f$.

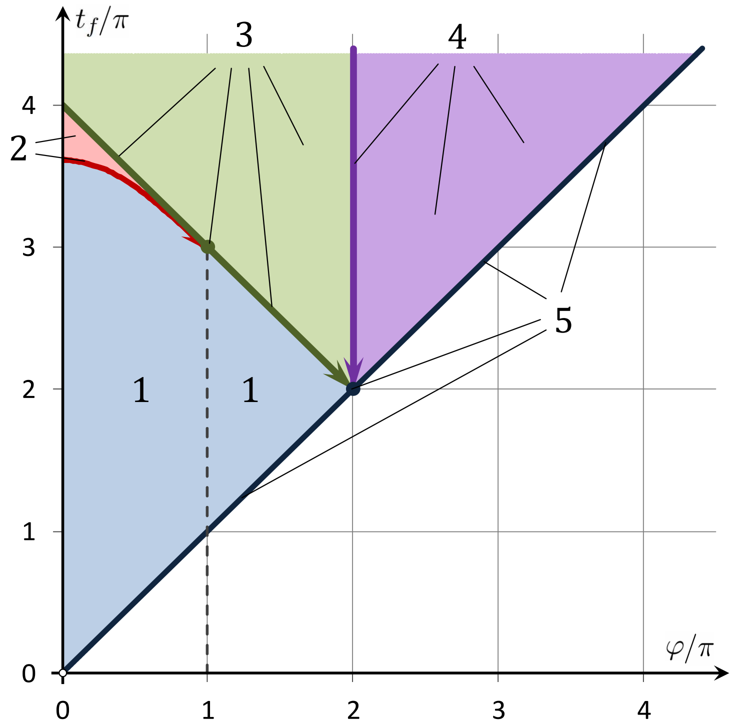

Fig. 7: Classification of φ-sections of the reachable set $G(t_f)$ for values $t_f > 0$ and $0 \leqslant \varphi \leqslant t_f$

In Case 5, as noted in Section II.A, any φ-section is a one-point set. Geometric coordinates in the original system are represented by the formulas $x(t_f) = \sin t_f$ and $y(t_f) = 1 - \cos t_f$. Position of such a point in the auxiliary coordinate system has the form $X(t_f) = 0$, $Y(t_f) = 0$.

In the following Sections, we describe the φ-sections for Cases $1-4$.

VI Boundary of φ-sections for Case 1

We assume that φ and t_f correspond to Case 1. The curves A1, A2, A3, and A6 are used as the basic elements of the boundary of the φ-sections. Each of them is fully included into the description of the boundary. This case is partially considered in [45] where it was assumed that $t_f \leqslant 2\pi$.

From the first two relations in (22), it follows that $0 \leqslant \varphi < 2\pi$ and $0 < \theta < 2\pi$, where $\theta = (t_f - \varphi)/2$. Considering formulas (10), (13) for the curves A1 and A6 (they are the arcs of circumferences), as well as, the corresponding ranges of parameters s_1 and s_3 in (4), we conclude that in Case 1, the span of each of the arcs A1 and A6 is less than 2π.

If $\varphi = 0$, then the arc A1 degenerates into a point coinciding with the starting point of the curve A3 and the end point of the curve A2. If $\varphi > 0$, the arc A1 is not degenerate. Its starting point is below the axis X, and its end point is above the axis X.

1) Consider the curve A3. For the extreme values $s_3 = 0$ and $s_3 = \theta$, we have

$$Y_{U3}(0) = (t_f - \varphi)\sin\left(\frac{\varphi}{2}\right) \geqslant 0, \qquad Y_{U3}(\theta) = 4\sin\left(\frac{t_f - \varphi}{4}\right)\sin\left(\frac{t_f + \varphi}{4}\right) > 0. \tag{29}$$

The first inequality follows from the fact that $\varphi \in [0, 2\pi)$ and $\varphi < t_f$. Using the condition $t_f < 4\pi - \varphi$, we obtain the second inequality. The first inequality turns into equality only for $\varphi = 0$. Analyzing the derivative of the function $Y_{U3}(s_3)$ w.r.t. s_3, we establish that $Y_{U3}(s_3) > 0$ for any $s_3 \in (\,0,\, \theta\,)$ (see Fig. 8).

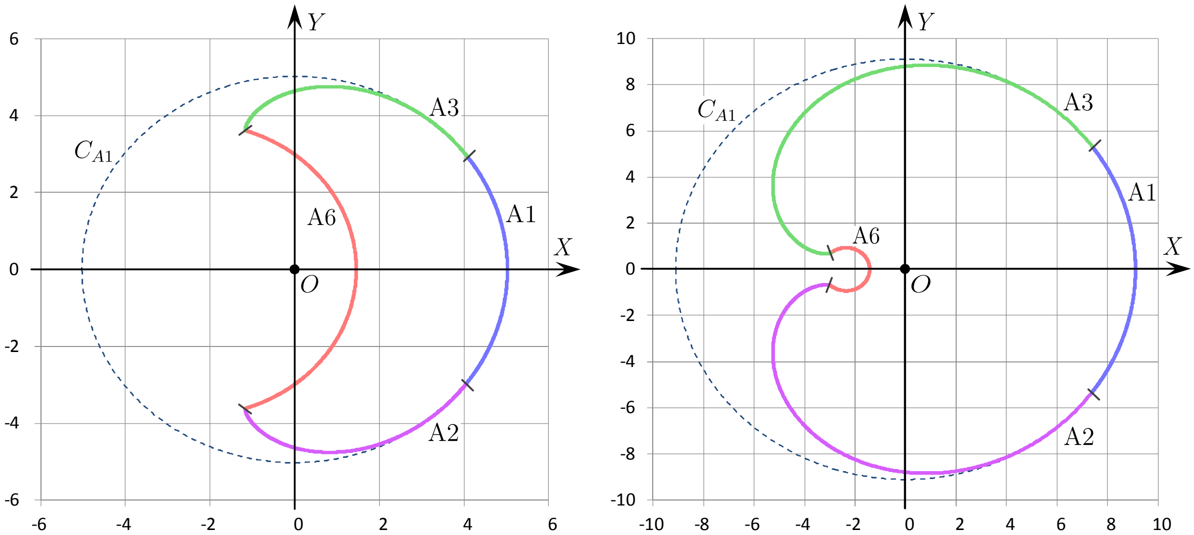

Fig. 8: Variants of the sets $G_\varphi(t_f)$ for Case 1 with $\varphi = 0.4\pi$ and two values $t_f = 2\pi$ (left) and $t_f = 3.3\pi$ (right)

Thus, in Case 1, the curve A3 lies above the axis X (excepting the initial point at $\varphi = 0$). The curve A2 is symmetric to the curve A3 w.r.t. the axis X. For $\varphi = 0$, the curves A2 and A3 have a point of their mutual joining (it is located on the axis X), which coincides with the degenerate point of the arc A1.

2) In general, taking into account the results of Section 2, we see that the "glued" curve $\mathrm{A}_\varphi(t_f) = \mathrm{A1} \cup \mathrm{A3} \cup \mathrm{A6} \cup \mathrm{A2}$ is a piecewise smooth closed one without self-intersections. The smoothness is broken only at the points of joining the arcs A2 and A3 with the arc A6. The glued curve contains *all* points of motion by the controls $U1$, $U2$, $U3$, and $U6$ for given t_f and φ.

Let us denote by the symbol $M_\varphi(t_f)$ the closed set bounded by the curve $\mathrm{A}_\varphi(t_f)$. By Lemma 5, this curve belongs to $\partial G_\varphi(t_f)$ and the inclusion $G_\varphi(t_f) \subset M_\varphi(t_f)$ is true.

For $\varphi \in (0, t_f)$, consider the motion generated on the interval $[0, t_f]$ by the constant control $u(t) \equiv \varphi/t_f$. Such a motion does not satisfy the PMP. Therefore, by virtue of [43], it leads to $\mathrm{int}G(t_f)$, and, hence, to $\mathrm{int}G_\varphi(t_f)$. For $\varphi = 0$, as a similar motion (but with one switch), we take the motion with the control $u(t) = -0.5$ for $t \in [0, t_f/2)$ and $u(t) = +0.5$ for $t \in [t_f/2, t_f]$. It also leads into $\mathrm{int}G_\varphi(t_f)$. Turning to Lemma 7, we see that for the set $M = \mathrm{int}M_\varphi(t_f)$ all lemma conditions are satisfied. Therefore, $\mathrm{int}M_\varphi(t_f) \subset G_\varphi(t_f)$.

As a result, we get $M_\varphi(t_f) = G_\varphi(t_f)$.

Variants of the sets $G_\varphi(t_f)$ for Case 1 are shown in Fig. 8. Scale of the image is determined by the radius of the circle C_{A1}.

VII Boundary of φ-sections for Case 2

We fix φ and t_f satisfying the conditions of Case 2. As in Case 1, the boundary of the φ-section will be constructed on the basis of the curves A1, A2, A3, and A6. The main feature is that any φ-section related to Case 2 is not simply connected.

VII.A Analysis of arcs of the curves A2 and A3 between the points of their intersection

Each of the curves A2 and A3 is an involute arc. The curve A1 joins with the curves A2 and A3 with keeping of curvature continuity (Section II.G, Property 7).

For $\varphi > 0$ and basing on (23), we can show that the curves A2 and A3 have one point of intersection (with tangency) under the condition

$$t_f = 3\pi + 2\cos(\varphi/2), \tag{30}$$

and two intersection points under the condition

$$t_f > 3\pi + 2\cos(\varphi/2). \tag{31}$$

For $\varphi = 0$, the only difference is in the presence of an additional common point on the axis X due to the degeneration of the A1 curve.

The situations corresponding to the conditions of tangency (30) and intersection (31) of the curves A2 and A3 are illustrated in Fig. 9.

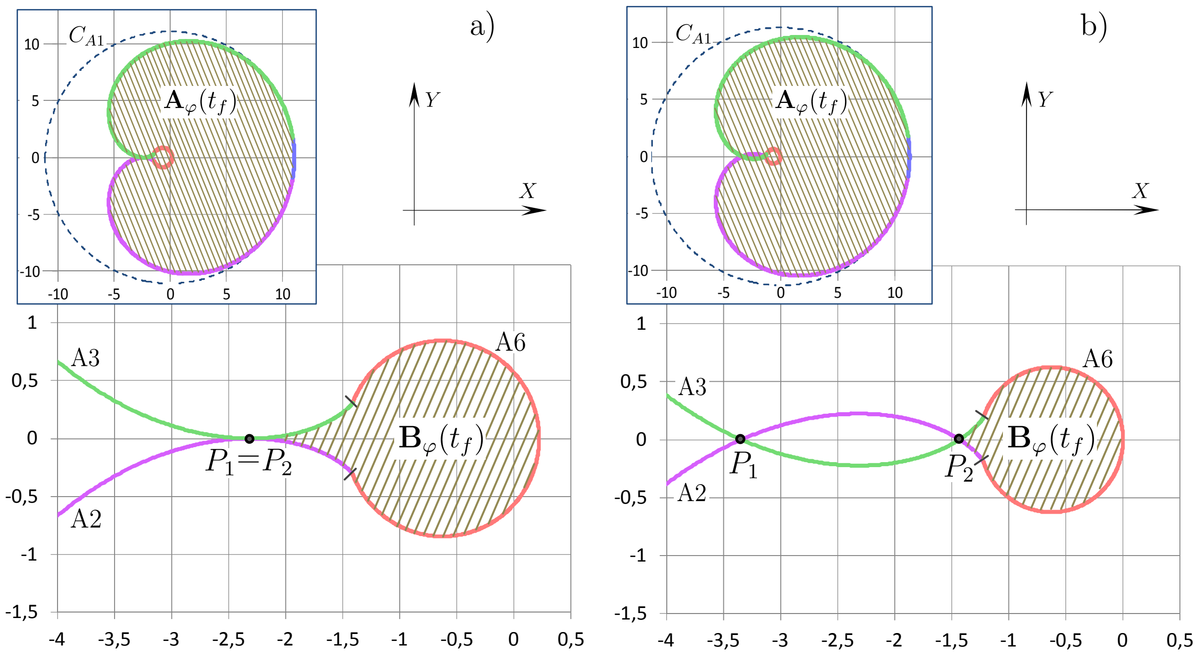

Fig. 9: The sets $\mathbf{A}_\varphi(t_f)$ and $\mathbf{B}_\varphi(t_f)$ for Case 2 with $\varphi = 0.1\pi$ and with two values t_f: a) $t_f = 3\pi + 2\cos(0.05\pi)$, b) $t_f = 3.7\pi$

Consider under condition (31) an open arc of the curve A3 between the points P_1 and P_2 in the plane X, Y. This arc is located below the axis X. Let us show that it belongs to $\mathrm{int}G_\varphi(t_f)$. We shall use Lemma 4. To ensure that the conditions of this Lemma are fulfilled, we establish that for any point $\mathcal{P}$ of this arc the corresponding motion (with a control of the type $U3$) has no cycles and each of the three intervals of the control constancy is not degenerate.

For controls of the type $U3$, the switching times t_1 and t_2 satisfy the relation $\varphi = t_1 - (t_f - t_2)$. The sum of the lengths of the first and third intervals does not exceed t_f, therefore, $2t_1 - \varphi = t_1 + (t_f - t_2) \leqslant t_f$. For Case 2 (see (23)), the inequality $t_f < 4\pi - \varphi$ holds. Therefore, $2t_1 - \varphi < 4\pi - \varphi$, i.e., $t_1 < 2\pi$. It means that there are no cycles on the first interval. For $\varphi \geqslant 0$, the length of the third interval does not exceed the length of the first one. So, there are no cycles on the third interval also.

As noted in Section II.G, Property 4, none of the regions of constancy of control of the type $U3$ leading to an inner point of the arc A3 is degenerate. Applying Lemma 4, we obtain $(\mathcal{P}, \varphi)^{\mathsf{T}} \in \mathrm{int}G(t_f)$. Hence, $\mathcal{P} \in \mathrm{int}G_\varphi(t_f)$.

VII.B Description of the boundary of φ-sections for Case 2 in the form of outer and inner contours

The curve A6 is a circular arc. Its center (in the auxiliary coordinate system) is located at the point H by formula (15), and the radius R_{A6} is described by formula (16). From the second inequality in the definition of Case 2, it follows that the arc A6 is non-degenerate (the radius is not equal to zero).

The arc A6 (with parts of the curves A2 and A3 attached to it up to the second point P_2 of their intersection) forms a closed curve. Let us denote it by $\mathrm{B}_\varphi(t_f)$. The symbol $\mathrm{A}_\varphi(t_f)$ denotes a closed curve composed of the arc A1 with parts of the curves A2 and A3 attached to it at the first point P_1 of their intersection (see Fig. 9). When $\varphi = 0$, the arc A1 degenerates into a point that becomes the junction point of the curves A2 and A3. Therefore, for $\varphi = 0$, we can assume that the closed curve $\mathrm{A}_\varphi(t_f)$ is formed by two curves A2 and A3 (up to the point P_1). Each of the curves $\mathrm{A}_\varphi(t_f)$ and $\mathrm{B}_\varphi(t_f)$ has no self-intersections. Let $\mathbf{A}_\varphi(t_f)$ (respectively, $\mathbf{B}_\varphi(t_f)$) be a closed set bounded by the curve $\mathrm{A}_\varphi(t_f)$ (respectively, curve $\mathrm{B}_\varphi(t_f)$).

The sets $\mathbf{A}_\varphi(t_f)$ and $\mathbf{B}_\varphi(t_f)$ are shown in Fig. 9.

When fulfilling inequality (31), the arcs of the curves A2 and A3 between the points P_1 and P_2 of their intersection lie in $\mathrm{int}G_\varphi(t_f)$.

1) Consider two circles centered at the point H: one passes through the point P_1, the other through the point P_2. The corresponding circles will be denoted by C_{P1} and C_{P2}. In Section II.G (Properties 5 and 6), it was noted that for the parametrically defined curves A2 and A3, there is a monotonic change of the distance from the point H to the points of the curves A2 and A3. From this, it follows that the circle C_{A6} with the center H, on the boundary of which the curve A6 lies, belongs to the set $\mathbf{B}_\varphi(t_f)$. Besides, for (31), the circle C_{P1} covers the circle C_{P2}, and for (30), these circles coincide.

Additionally, taking into account Property 10 of Section II.G, we get that the curve $\mathrm{A}_\varphi(t_f)$ (excepting the point P_1) lies outside the circle C_{P1}. The remaining parts of the curves A2, A3, and, also, the curve A6 are located in $\mathrm{int}C_{P1}$. Similarly, the curve $\mathrm{B}_\varphi(t_f)$ (excepting the point P_2) lies in $\mathrm{int}C_{P2}$; the remaining parts of the curves A2, A3, and the whole curve A1 are outside the circle C_{P2}.

Outside the set $\mathbf{A}_\varphi(t_f)$, there are no points generated by controls of the types $U1$, $U2$, $U3$, and $U6$. Therefore, by virtue of Lemma 5 the curve $\mathrm{A}_\varphi(t_f)$ forms the "outer" boundary of the set $G_\varphi(t_f)$ for Case 2.

2) Now, let us establish that the curve $\mathrm{B}_\varphi(t_f)$ is the "inner" boundary of the set $G_\varphi(t_f)$.

2.1) Consider in the set $\mathrm{int}\mathbf{B}_\varphi(t_f)$ a point J located on the axis X and spaced from the point H to the left by $\frac{1}{2}R_{A6}(t_f)$. We have

$$J = \left(-4\sin\left(\frac{\varphi}{2}\right) - 2\sin\left(\frac{t_f+\varphi}{4}\right),\ 0\right)^{\mathsf{T}}.$$

We shall show that $J \notin G_\varphi(t_f)$. Suppose the opposite, *i.e*, $J \in G_\varphi(t_f)$. Then by Filippov's theorem [51], there is an *time-optimal* control leading to the phase point $(J,\varphi)^{\mathsf{T}}$. Let t_f^* be the corresponding time-optimal instant. We have $0 \leqslant t_f^* \leqslant t_f$.

By virtue of Theorem 1 of [1, p. 515], the time-optimal control can be taken in the form of one of six variants $U1 - U6$. Let us consider them. At the same time, for the $U5$ and $U6$ control types, we do not suppose obligatory to fulfill condition (2).

A control of the type $U4$ gives the value $\varphi \leqslant 0$ at the instant t_f^*. Since we investigate the case $0 \leqslant \varphi < \pi$, then for $U4$, we should consider only the case of $\varphi = 0$ with the control $u(\cdot) \equiv 0$. Here, we get the point $\big(x(t_f^*), y(t_f^*)\big)^{\mathsf{T}} = \big(t_f^*, 0\big)^{\mathsf{T}}$. It does not coincide with the point J for any $t_f^* \in [0, t_f]$.

To provide the inequality $\varphi > 0$ at the instant t_f^* with a control of the type $U5$, it is required that the length of the middle interval of the control constancy to be less than the sum of the lengths of the first and third intervals. In paper [41] (the proof of Lemma 2) for such a condition, it was established that there is another motion that comes exactly to the same phase point at the same instant t_f^*, but it does not satisfy the PMP. So, the instant t_f^* is not time-optimal. Thus, the controls of the type $U5$ cannot be time-optimal to arrive to the point $(J,\varphi)^{\mathsf{T}}$ for $\varphi > 0$.

If $\varphi = 0$, then controls of the type $U5$ generate the same set of points (x, y) at the instant t_f^* as controls of the type $U6$. Therefore, controls of the type $U5$ need not be considered.

Controls of four types remain: $U1$, $U2$, $U3$, and $U6$. Let us introduce the notations A1*, A2*, A3*, and A6* for the curves generated by the indicated controls at the time-optimal instant $t_f^* \in [\varphi, t_f]$ with the fixed value φ. These curves are calculated using formulas (10)–(13) and (4) with the t_f symbol replaced by t_f^* one. Let us show that curves A1*, A2*, A3*, and A6* do not contain the point J.

Consider two variants: $t_f^* \in [\varphi, \pi)$, $t_f^* \in [\pi, t_f]$.

In the first variant, you can make sure that the curves A1*, A2*, A3*, and A6* are located in the half-plane $X \geqslant 0$. At the same time, the point J is in the half-plane $X < 0$. Therefore, any controls of the types $U1$, $U2$, $U3$, and $U6$ cannot be the solution of the time-optimal problem for t_f^*.

In the second variant, the inequality $\pi/4 \leqslant (t_f^* + \varphi)/4$ is true. We show that $J \in \mathrm{int}C_{A6^*}$. To do this, it is enough to establish that the distance $2\sin((t_f+\varphi)/4)$ between the points J and H is less than the radius $R_{A6}(t_f^*) = 4\sin\big((t_f^*+\varphi)/4\big)$ of the circumference corresponding to the arc A6* (see (16)). The modulus sign in the formula for $R_{A6}(t_f^*)$ is omitted, since by virtue of $0 \leqslant t_f^* + \varphi \leqslant t_f + \varphi < 4\pi$, the inequality $\sin\big((t_f^*+\varphi)/4\big) \geqslant 0$ is fulfilled.

So, let us check the inequality

$$2\sin((t_f+\varphi)/4) < 4\sin\big((t_f^*+\varphi)/4\big). \tag{32}$$

If $(t_f^*+\varphi)/4 \geqslant \pi/2$, then inequality (32) is satisfied due to the monotonicity of the sine for the values $\pi/2 \leqslant (t_f^*+\varphi)/4 \leqslant (t_f+\varphi)/4 < \pi$. The last inequality follows from the definition of Case 2. If $(t_f^* + \varphi)/4 < \pi/2$, then $4\sin\big((t_f^* + \varphi)/4\big) \geqslant 4\sin(\pi/4) = 2\sqrt{2}$. From here, taking into account $2\sin((t_f + \varphi)/4) \leqslant 2$, inequality (32) follows.

Since the arc A6* lies on the boundary of the circle C_{A6^*}, any control of the type $U6$ cannot lead to the phase point $(J,\, \varphi)^\mathsf{T}$ at the instant t_f^*.

From Section II.G, Property 9, it follows that the curves A1*, A2*, and A3* are located outside $\mathrm{int}C_{A6^*}$. Therefore, controls of the types $U1$, $U2$, and $U3$, also, cannot lead to the phase point $(J,\, \varphi)$ at the instant t_f^*.

Thus, none of controls of the types $U1$–$U6$ can give solutions to the time-optimal problem to the point $(J,\, \varphi)$ at the instant t_f^*. Therefore, the instant $t_f^* \in [0,\, t_f]$ cannot be the time-optimal instant. We came to a contradiction. Therefore, $J \notin G_\varphi(t_f)$.

2.2) As noted above, the curve $B_\varphi(t_f)$ (excepting the point P_2) is located in $\mathrm{int}C_{P2}$. Besides the curve $B_\varphi(t_f)$, there are no other points in this circle formed by controls of the types $U1$, $U2$, $U3$, and $U6$. So, in the set $\mathrm{int}\mathbf{B}_\varphi(t_f)$, there are no points generated by these controls for the considered values t_f and φ.

Using Lemma 6, we see that all its conditions are fulfilled. We get that the curve $B_\varphi(t_f)$ forms the "inner" boundary of the φ-section of the set $G(t_f)$ for Case 2.

Consider the open set $M_\varphi(t_f) = (A_\varphi(t_f))^- \cap (B_\varphi(t_f))^+$. The curves $\mathrm{A}_\varphi(t_f)$ and $\mathrm{B}_\varphi(t_f)$ have at most one common point. Such a point is one of tangency of the curves A2 and A3 under condition (30). If this condition is not true, then the curves $\mathrm{A}_\varphi(t_f)$ and $\mathrm{B}_\varphi(t_f)$ have not the common points. Based on the Jordan and Schoenflies theorems [49, 50], it can be shown that the set $M_\varphi(t_f)$ is connected.

Thus, the conditions of Lemma 7 are satisfied for the set $M = \mathrm{int}M_\varphi(t_f)$. And we conclude that the set $G_\varphi(t_f)$ in Case 2 has the external boundary in the form of the curve $\mathrm{A}_\varphi(t_f)$ and the inner boundary in the form of the curve $\mathrm{B}_\varphi(t_f)$. We have $G_\varphi(t_f) = \mathbf{A}_\varphi(t_f) \backslash \mathrm{int}\mathbf{B}_\varphi(t_f)$ (Fig. 9).

VIII Boundary of φ-sections for Case 3

The peculiarity of Case 3 is that the curve A6 will not be used in the description of the boundary of the φ-section. To construct the boundary, some partition of the curves A2 and A3 will be required.

VIII.A Partition of the curves A2 and A3

The required partition of the curve A3 is described below in three sub-points. Due to the symmetry about the axis X, the similar partition takes place for the curve A2.

1) The curve A3 is defined by formula (12) and given with the help of the parameter $s_3 \in [0, \theta]$. Let us put $s_3^c = 2\pi - \varphi$. Now, we show that $s_3^c \in (0, \theta]$. Indeed, it follows from the inequality $\varphi < 2\pi$ in the definition of Case 3 that $s_3^c > 0$. The second relation in the definition of Case 3 is written as $t_f - \varphi \geqslant 4\pi - 2\varphi$. Therefore, $s_3^c \leqslant (t_f - \varphi)/2 = \theta$. Thus, the value $s_3 = s_3^c$ defines some point on the curve A3, which we denote $\mathcal{P}_3^c$. The point $\mathcal{P}_3^c$ does not coincide with the starting point of the curve A3, but it may coincide with the curve last point.

Meaningfully, the parameter s_3^c corresponds to the value $t_1 = 2\pi$ (by virtue of (3)). Therefore, there is a cycle in the first constancy interval of control of the type $U3$. For $s_3 < s_3^c$, the resulting motion does not contain cycles. For $s_3 > s_3^c$, the duration of the first interval is $t_1 > 2\pi$; from here, the first interval contains at least one cycle.

In Fig. 10, the curve A3 corresponding to $t_f = 3.5\pi$ and $\varphi = 1.2\pi$ is shown. Dashed trajectories are built for the five values of the parameter s_3: 0, 0.22θ, 0.44θ, s_3^c, θ. Here, $\theta = 1.15\pi$. The trajectory leading to the point $\mathcal{P}_3^c$ corresponds to the value $s_3^c = 0.8\pi$. For $s_3 \in [0, 0.8\pi)$, the first interval of the control constancy has the duration less than 2π. For $s_3 \in (0.8\pi, 1.15\pi]$, the first interval of the control constancy is greater than 2π.

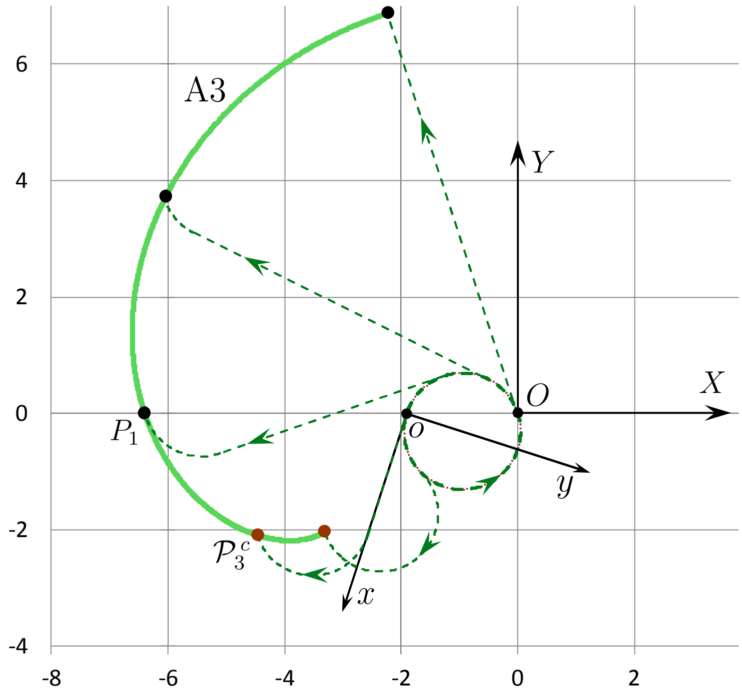

Fig. 10: Example of the point $\mathcal{P}_3^c$ location on the curve A3 for $t_f = 3.5\pi$ and $\varphi = 1.2\pi$

There may be cycles on the third interval of the control constancy, but then there should be also a cycle on the first interval, since $\varphi = t_1 - (t_f - t_2) \geqslant 0$.

An important property is that the point $\mathcal{P}_3^c$ cannot lie above the straight line X, i.e., $Y_{U3}(s_3^c) \leqslant 0$. This follows from the substitution of the value $s_3^c = 2\pi - \varphi$ in (12) and analysis of the second coordinate $Y_{U3}(s_3^c)$ with taking into account the condition $t_f \geqslant 4\pi - \varphi$ from (24). The equality $Y_{U3}(s_3^c) = 0$ is equivalent to the fulfillment of at least one of the conditions $\varphi = 0$, $t_f = 4\pi - \varphi$.

2) From the definition of Case 3, it follows that $t_f \geqslant 2\pi$. Thus, in Case 3, the relations $0 \leqslant \varphi < 2\pi$, $\varphi < t_f$ hold. Therefore, the first inequality from (29) (established for Case 1) is valid. This means that the starting point $\mathcal{P}_{1,3}$ of the curve A3 is above the axis X (for $\varphi > 0$), or on this axis (for $\varphi = 0$).

Consider a part of the curve A3 from the starting point $\mathcal{P}_{1,3}$ to the point $\mathcal{P}_3^c$. We establish that on this part there is a point P_1, lying on the axis X, such that the open arc $(\mathcal{P}_{1,3}, P_1)$ is located above the axis X, and then, the open arc $(P_1, \mathcal{P}_3^c)$ is below the axis X. The point P_1 can coincide with the point $\mathcal{P}_3^c$.

3) If the point $\mathcal{P}_3^c$ does not coincide with the point P_1, then consider an open arc $(P_1,\ \mathcal{P}_3^c)$ of the curve A3. For any point $\mathcal{P}$ of this arc, a control of the type $U3$ leading to it has three non-degenerate intervals of control constancy (see Section II.G, Property 4). The corresponding trajectory has no cycles by definition of the point $\mathcal{P}_3^c$. The arc $(P_1,\ \mathcal{P}_3^c)$ lies below the axis X. By Lemma 4, we see that the point $(\mathcal{P}, \varphi)^{\mathsf{T}}$ belongs to $\mathrm{int}G(t_f)$.

VIII.B Non-degenerate and degenerate subcases

We shall distinguish two subcases:

$$t_f > 4\pi - \varphi, \tag{33}$$

$$t_f = 4\pi - \varphi. \tag{34}$$

The first one will be called non-degenerate, the second is degenerate.

1) Non-degenerate subcase. Rewrite condition (33) as $t_f - \varphi > 4\pi - 2\varphi$. Then, it follows that the point $\mathcal{P}_3^c$ defined by the parameter $s_3^c = 2\pi - \varphi$ does not coinside with the point $\mathcal{P}_{3,6}$ corresponding to the parameter $s_3 = \theta$. Consider the half-open arc $[\mathcal{P}_3^c,\, \mathcal{P}_{3,6})$ of the curve A3. A control of the type $U3$ leading to any point $\mathcal{P}$ of this arc has three non-degenerate intervals of control constancy. Moreover, the first interval contains a cycle due to the choice of the point $\mathcal{P}_3^c$. By Lemma 2, we obtain that $(\mathcal{P},\, \varphi)^\mathsf{T} \in \mathrm{int}G(t_f)$.

Thus, the arc $(P_1,\, \mathcal{P}_3^c) \cup [\mathcal{P}_3^c,\, \mathcal{P}_{3,6})$ is located in $\mathrm{int}G_\varphi(t_f)$.

The last point $\mathcal{P}_{3,6}$ of the curve A3 is simultaneously the extreme point of the curve A6.

Consider the curve A6. Take an arbitrary point $\mathcal{P}$ on it. For the switching instants t_1 and t_2 of control of the type $U3$, which leads to this point, the following relations hold:

$$t_f = (t_1 - t_0) + (t_2 - t_1) + (t_f - t_2), \qquad \varphi = -(t_1 - t_0) + (t_2 - t_1) - (t_f - t_2).$$

Substituting these expressions into the inequality $t_f > 4\pi - \varphi$, we get $(t_2 - t_1) > 2\pi$. Therefore, the length of the middle interval of the control $U6$ constancy is greater than 2π. From the condition $\varphi < t_f$ satisfied to Case 3 (see (24)), it follows that the first and third intervals of control constancy cannot simultaneously degenerate.

Using Lemma 3, we obtain $(\mathcal{P}, \varphi)^\mathsf{T} \in \mathrm{int}G(t_f)$. Therefore, $\mathcal{P} \in \mathrm{int}G_\varphi(t_f)$. Thus, the whole curve A6 belongs to $\mathrm{int}G_\varphi(t_f)$.

For case (33), we get the following result. The curve A1 together with the part of the curve A3 (from the point $\mathcal{P}_{1,3}$ to the point P_1) and the part of the curve A2 (from the point P_1 to the point $\mathcal{P}_{1,2}$) form a closed curve without self-intersections. Denote it as $\mathrm{A}_\varphi(t_f)$. Let $\mathbf{A}_\varphi(t_f)$ be a closed set bounded by this curve. The curve A6 and the remaining parts of the curves A2, A3 belong to the set $\mathrm{int}\mathbf{A}_\varphi(t_f)$, and they are also in $\mathrm{int}G_\varphi(t_f)$.

Figure 4b in Section 2 refers to Case 3, non-degenerate subcase. It can be seen that the curve A3 after the first crossing the axis X (point P_1) makes several revolutions. The part of this curve after the point P_1 lies in $\mathrm{int}G_\varphi(t_f)$. Similarly, the same takes place for the part of the curve A2 symmetric to A3.

2) Degenerate subcase. From condition (34) and by analogy with the non-degenerate subcase, it follows that $\mathcal{P}_3^c = \mathcal{P}_{3,6}$. In this case, the curve A6 degenerates (the radius of the circle becomes equal to zero) into the point $H = \mathcal{P}_{2.6} = \mathcal{P}_{3.6}$. If $\varphi = 0$, then the curve A1 degenerates into a point coinciding with the points $\mathcal{P}_{1,2}$ and $\mathcal{P}_{1,3}$.

For the degenerate subcase in Fig. 11, the curve $\mathrm{A}_\varphi(t_f)$ composed of the curves A1, A3, A6 (degenerate curve), and A2 is shown. The point $\mathcal{P}_3^c$ coincides with the point H. Three variants are presented here: $\varphi = 0.3\pi$, $t_f = 3.7\pi$ (Fig. 11a); $\varphi = 1.0\pi$, $t_f = 3.0\pi$ (Fig. 11b); $\varphi = 1.4\pi$, $t_f = 2.6\pi$ (Fig. 11c).

2.1) Suppose that $\varphi < \pi$ (Fig. 11a). Then $P_1 \neq \mathcal{P}_{3,6}$. As in the non-degenerate case, the curve A1 together with a part of the curve A3 (from the point $\mathcal{P}_{1,3}$ to the point P_1) and a part of the curve A2 (from the point P_1 to the point $\mathcal{P}_{1,2}$) form a closed curve without self-intersections. Let $\mathbf{A}_\varphi(t_f)$ be a closed set bounded by this curve. Under this,

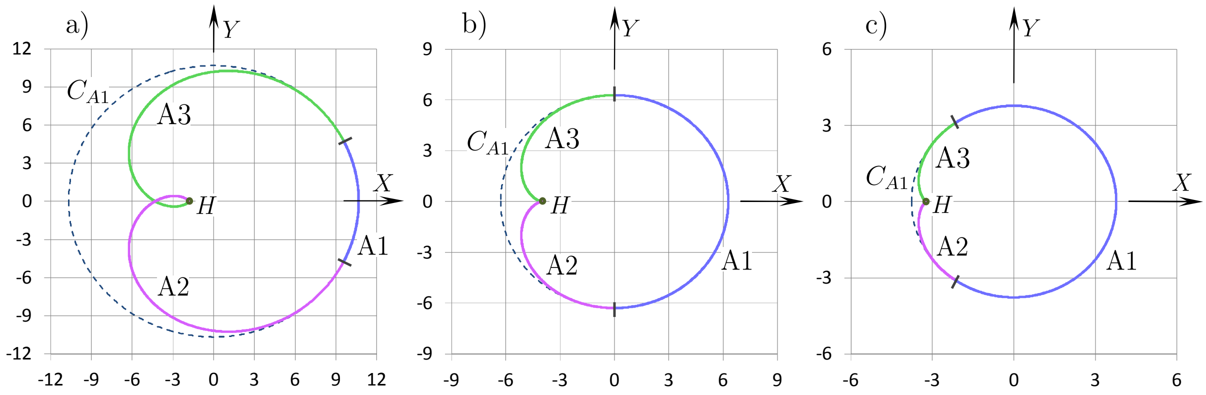

Fig. 11: Case 3. Variants of the curve $\mathrm{A}_\varphi(t_f)$ for the degenerate subcase

the arc $(\mathcal{P}_{2,6}, P_1)$ of the curve A2 and the arc $(P_1, \mathcal{P}_{3,6})$ of the curve A3 are in $\mathrm{int}G_\varphi(t_f)$. The similar property for the point $\mathcal{P}_{2.6} = \mathcal{P}_{3.6}$ has not yet been established.

2.2) Suppose $\varphi \geqslant \pi$. Then, $P_1 = \mathcal{P}_{3,6}$. We get that the curves A1, A2, and A3 form a closed curve without self-intersections. Let $\mathbf{A}_\varphi(t_f)$ be a closed set bounded by this curve.

Geometrically, the cases $\varphi = \pi$ (Fig. 11b) and $\varphi > \pi$ (Fig. 11c) differ: in the first of them, the curves A2 and A3 touch at the point $H = P_1$, and in the second situation, they join at this point at some angle.

Outside the set $\mathbf{A}_\varphi(t_f)$, as well as, in its interior, there are no points generated by controls of the types $U1$, $U2$, $U3$, and $U6$.

VIII.C Constructing the boundary of φ-section

Applying Lemma 5 to the set $\mathbf{A}_\varphi(t_f)$ introduced in the previous Section VIII.B, we obtain that

$$G_\varphi(t_f) \subset \mathbf{A}_\varphi(t_f), \qquad \partial\mathbf{A}_\varphi(t_f) \subset \partial G_\varphi(t_f). \tag{35}$$

Let us show that for the set $\mathrm{int}\mathbf{A}_\varphi(t_f)$, the conditions of Lemma 7 are satisfied. We put $M_\varphi(t_f) = \mathrm{int}\mathbf{A}_\varphi(t_f)$.

In the non-degenerate subcase, all arcs of the curves A2, A3, and A6 that do not participate in formation of boundary of the set $\mathbf{A}_\varphi(t_f)$ belong to the set $M_\varphi(t_f)$. Moreover, these arcs belong to $\mathrm{int}G_\varphi(t_f)$. Therefore, condition 2) of Lemma 5 is satisfied.

In the degenerate subcase for $\varphi < \pi$, condition 2) of Lemma 7 is satisfied. Indeed, for the parts of the curves A2, A3, and A6 that belong to the set $M_\varphi(t_f)$, it has been established that any point of them excepting, perhaps, only the point $\mathcal{P}_{3,6}$, belongs to $\mathrm{int}G_\varphi(t_f)$. For $\varphi \geqslant \pi$ there are no the curves A1, A2 A3, and A6 outside the set $\mathbf{A}_\varphi(t_f)$, and, therefore, in $M_\varphi(t_f)$. To apply Lemma 7 (under condition 1)), it is necessary to specify a point belonging to $\mathrm{int}G_\varphi(t_f)$. As such a point, the same one as in Section VI, take the point generated by the constant control $u(t) \equiv \varphi/t_f$. Thus, condition 1) of Lemma 7 is satisfied.

As a result, for all the variants (considered in Section VIII.B) of Case 3, we obtain the fulfillment of Lemma 7 conditions. So, $M_\varphi(t_f) = \mathrm{int}\mathbf{A}_\varphi(t_f) \subset G_\varphi(t_f)$. Hence, taking into account (35), we get $G_\varphi(t_f) = \mathbf{A}_\varphi(t_f)$ in Case 3.

The boundary of the set $G_\varphi(t_f)$ is made up of the curve A1, the part of the curve A3 to the first point of its intersection with the axis X, as well as the part of the curve A2 that is symmetric to it (see Figs. 11 and 12). Fig. 12a (12b) corresponds to $t_f = 4.5\pi$, $\varphi = \pi$ ($t_f = 8.5\pi$, $\varphi = \pi$).

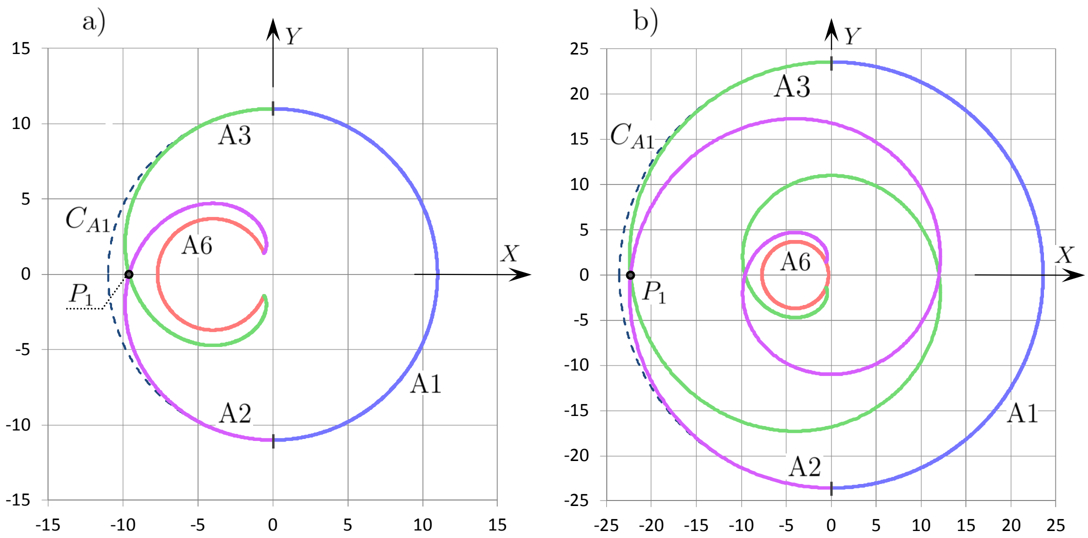

Fig. 12: Case 3. The set $G_\varphi(t_f)$ in the non-degenerate subcase

IX Boundary of φ-sections in Case 4

Let us show that in Case 4 any φ-section is the circle C_{A1} given by the curve A1. The position of the center of the circle depends on φ, and its radius depends on φ and t_f.

The curve A1 is defined by formula (10) and is an arc of a circle with the radius $R_{A1} = (t_f - \varphi)$ and with the center at the origin of the auxiliary coordinate system X, Y. By the definition of Case 4 (see (25)), the inequality $\varphi \geqslant 2\pi$ holds. The arc A1, the span of which is equal to φ, forms a circumference with an "overlap". The curves A2, A3, and A6 belong to the circle C_{A1}. Moreover, the points $\mathcal{P}_{1,2}$ and $\mathcal{P}_{1,3}$ (where the curves A2 and A3 are joining with the curve A1) lie on its boundary. All other points of the curves A2 and A3, as well as, all the curve A6 are located in intC_{A1} (Section II.G, Property 8).

Let us establish that all points of the curves A2, A3, and A6 lying in intC_{A1} belong to int$G_\varphi(t_f)$. The interior points of the curve A3 are generated by controls of the type $U3$ with three nondegenerate constancy intervals (Section II.G, Property 4). Here, the switching instans t_1 and t_2 are defined by the relation $\varphi = t_1 - (t_f - t_2)$. Since $\varphi \geqslant 2\pi$, so $t_1 > t_1 - (t_f - t_2) \geqslant 2\pi$. Therefore, on all motions leading to the inner points of the curve A3, there is a cycle on the first interval of control constancy. Thus, in accordance with Lemma 2, we obtain that the points of the curve A3 under consideration belong to int$G_\varphi(t_f)$. The similar property is valid for the curve A2.

Consider the curve A6. It is generated by controls of the type $U6$. The corresponding switching instans t_1 and t_2 are defined by the relations

$$t_f = (t_1 - t_0) + (t_2 - t_1) + (t_f - t_2), \qquad \varphi = -(t_1 - t_0) + (t_2 - t_1) - (t_f - t_2).$$

From here, $(t_2 - t_1) = (t_f + \varphi)/2$. From condition (25), we get $2\pi < (t_2 - t_1) < t_f$. Thus, for any point of the curve A6 on the corresponding control, the duration of the second interval is greater than 2π, and at least one of the two adjacent extreme intervals is not degenerate. By Lemma 3, we conclude that the curve A6 entirely belongs to int$G_\varphi(t_f)$.

Using Lemma 5 and Lemma 7, we obtain $G_\varphi(t_f) = C_{A1}$.

Figure 13a (13b) shows the set $G_\varphi(t_f)$ for the values $t_f = 5\pi$ and $\varphi = 2.5\pi$ (correspondingly, $t_f = 8\pi$ and $\varphi = 2.5\pi$). It coincides with the circle C_{A1}. The curve A1 is a circumference with an “overlap”. The curves A2, A3, and A6 are also shown.

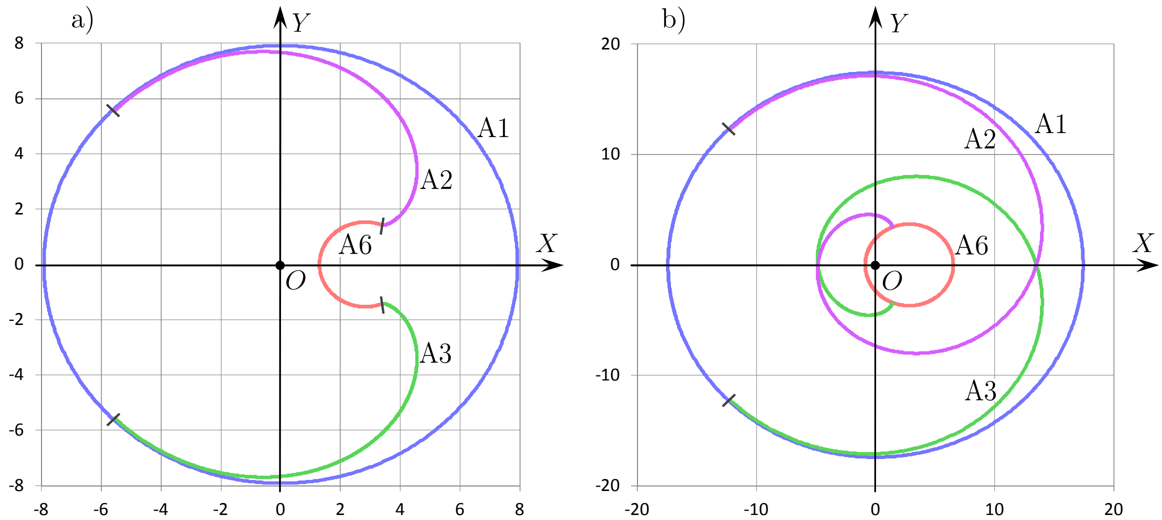

Fig. 13: Case 4. The set $G_\varphi(t_f)$ for two variants t_f and φ

X Case $\varphi < 0$

The study of the case $\varphi < 0$ is based on the symmetry property of system (1), which is the following. Consider the motion $(x^*(t), y^*(t), \varphi^*(t))^{\mathsf{T}}$ of the system on the interval $[0, t_f]$ from the initial zero phase point, generated by some admissible control $u^*(t)$. At the instant t_f, we get the point $(x^*(t_f), y^*(t_f), \varphi^*(t_f))^{\mathsf{T}}$. The control $u_*(t) = -u^*(t)$ (i.e., it differs from the initial one only in sign) with the same zero initial phase point gives the phase state $(x_*(t_f), y_*(t_f), \varphi_*(t_f))^{\mathsf{T}}$ at the instant t_f, where $x_*(t_f) = x^*(t_f)$, $y_*(t_f) = -y^*(t_f)$, $\varphi_*(t_f) = -\varphi^*(t_f)$.

This leads to the fact that the φ^*-section $G_{\varphi^*}(t_f)$ of the reachable set $G(t_f)$ for any φ^* is associated with the corresponding section for $\varphi_* = -\varphi^*$ by mirroring about the axis x of the original coordinate system. Within the framework of the auxiliary coordinate system (if it is also introduced for $\varphi < 0$), the new section coincides with the old one. Such facts make it possible not to consider separately the case $\varphi < 0$. The result for it is determined by the case $\varphi > 0$.

For $\varphi = 0$, the original coordinate system x, y coincides with the auxiliary system X, Y. Therefore, the corresponding φ-section $G_\varphi(t_f)$ is symmetric w.r.t. the axis x of the original coordinate system.

XI Conclusion

For the Dubins car with symmetric control constraint, the analytical description is obtained for the sections along the angular coordinate φ of the three-dimensional reachable set $G(t_f)$. Possible types of two-dimensional φ-sections of the set $G(t_f)$ with different collections of boundary arcs are classified. Relations are obtained that explicitly indicate the type of each φ-section for the given values φ and t_f. The case is highlighted when the φ-section is not simply connected.

The material in Sections V−X can be interpreted as a description of the additional conditions to definition of controls of the types $U1 - U6$. Such conditions (together with relation (2)) distinguish the controls leading to the boundary of the reachable set $G(t_f)$. These conditions depend on t_f and φ (see formulas (22)–(26) and Fig. 7). Taking them into account completely determines the boundary of the reachable set. It will open up the possibility (based on the effective numerical construction of the set $G(t_f)$ with the growth of t_f) to solve many problems of optimal control with the dynamics of the Dubins car including the time-optimal problems. It is also possible to use the results obtained in solving some game problems.

The paper results are planned to carry over onto the case of an asymmetric constraint on the control $u \in [u_1, u_2]$ for $u_1 < 0$, $u_2 > 0$.

Acknowledgments The authors are grateful to M.A. Patrakeev for consultations related to application of the Jordan and Schoenflies theorems.

References

[1] Dubins, L. E., "On Curves of Minimal Length with a Constraint on Average Curvature and with Prescribed Initial and Terminal Positions and Tangents," *American J. Math.*, Vol. 79, No. 3, 1957, pp. 497–516, doi:10.2307/2372560.

[2] Sussmann, H. J. and Tang, W., "Shortest Paths for the Reeds-Shepp Car: a Worked Out Example of the Use of Geometric Techniques in Nonlinear Optimal Control," Report sycon-91-lo, Rutgers University, 1991.

[3] Kaya, C. Y., "Markov-Dubins Path via Optimal Control Theory," *Computational Optimization and Applications*, Vol. 68, No. 3, 2017, pp. 719–747, doi: 10.1007/s10589-017-9923-8.

[4] Markov, A. A., "A Few Examples of Solving Special Problems on the Largest and Smallest Values," *The communications of the Kharkov mathematical society*, Vol. 1, No. 2, 1889, pp. 250–276. (in Russian).

[5] Isaacs, R., "Games of Pursuit," Tech. rep., RAND Corporation, Santa Monica, 1951.

[6] Miele, A., *Flight Mechanics, Volume 1: Theory of Flight Paths*, Addison-Wesley Publishing Company, London, 1962.

[7] Pecsvaradi, T., "Optimal Horizontal Guidance Law for Aircraft in the Terminal Area," *IEEE Trans. on Automatic Control*, Vol. 17, No. 6, 1972, pp. 763–772.

[8] Laumond, J.-P., ed., *Robot Motion Planning and Control*, Springer-Verlag, Berlin; Heidelberg, 1998, doi:10.1007/BFb0036069.

[9] Hernandez, J. D., Moll, M., Vidal, E., Carreras, M., and Kavraki, L. E., "Planning Feasible and Safe Paths Online for Autonomous Underwater Vehicles in Unknown Environments," in "2016 IEEE/RSJ International Conference on Intelligent Robots and Systems (IROS)," , 2016, pp. 1313–1320, doi:10.1109/IROS.2016.7759217.

[10] LaValle, S. M., *Planning Algorithms*, Cambridge University Press, 2006.

[11] Giordano, P. R. and Vendittelli, M., "Shortest Paths to Obstacles for a Polygonal Dubins Car," *IEEE Transactions on Robotics*, Vol. 25, No. 5, 2009, pp. 1184–1191, doi:10.1109/TRO.2008.2011421.

[12] Manyam, S., Rathinam, S., Casbeer, D., and Garcia, E., "Shortest Paths of Bounded Curvature for the Dubins Interval Problem," arXiv:1507.06980v2, 2015.

[13] Manyam, S. G., Casbeer, D. W., Moll, A. L., and Fuchs, Z., "Shortest Dubins Path to a Circle," in "AIAA SciTech 2019 Forum," San Diego, California, 2019, pp. 1–7, doi:10.2514/6.2019-0919.

[14] Chen, Z., "On Dubins Paths to a Circle," *Automatica*, Vol. 117, doi:10.1016/j.automatica.2020.108996.

[15] Zheng, Y., Chen, Z., Shao, X., and Zhao, W., "Time-Optimal Guidance for Intercepting Moving Targets with Impact-Angle Constraints," *Chinese Journal of Aeronautics*, doi:https://doi.org/10.1016/j.cja.2021.08.002.

[16] Koval, A. and Isler, V., "Turning a Corner with a Dubins Car," in "2019 International Conference on Robotics and Automation (ICRA)," , 2019, pp. 8570–8576, doi:10.1109/ICRA.2019.8794361.

[17] Lee, J. H., Cheong, O., Kwon, W. C., Shin, S. Y., and Chwa, K. Y., "Approximation of Curvature-Constrained Shortest Paths through a Sequence of Points," in Paterson, M. S., ed., "Algorithms - ESA 2000," Springer, Berlin, Heidelberg, 2000, pp. 314–325, doi:10.1007/3-540-45253-2_29.

[18] Berdyshev, Y. I., "On the Problem of Sequential Traversal of a Set of Smooth Manifolds by a Nonlinear Controlled Object," *Differential Equations*, Vol. 38, No. 11, 2002, pp. 1541–1552, doi:10.1023/A:1023676619449.

[19] Chen, Z. and Shima, T., "Shortest Dubins Paths through Three Points," *Automatica*, Vol. 105, 2019, pp. 368–375.

[20] Berdyshev, Y. I., "Optimal Control in a Nonlinear Sequential Rendezvous Problem," *Journal of Computer and Systems Sciences International*, Vol. 58, No. 1, 2019, pp. 95–104.

[21] Chen, Z., Wang, K., and Lu, Y., "Elongation Of Curvature-Bounded Path," arXiv:2109.02125v1, 2021.

[22] Mitchell., I. M., Bayen, A. M., and Tomlin, C. J., "A Time-Dependent Hamilton-Jacobi Formulation of Reachable Sets for Continuous Dynamic Games," *IEEE Transactions on Automatic Control*, Vol. 50, No. 7, 2005, pp. 947–957, doi:10.1109/TAC.2005.851439.

[23] Meyer, Y., Isaiah, P., and Shima, T., "On Dubins Paths to Intercept a Moving Target," *Automatica*, Vol. 53, 2015, pp. 256–263, doi:10.1016/j.automatica.2014.12.039.

[24] Buzikov, M. E. and Galyaev, A. A., "Time-Optimal Interception of a Moving Target by a Dubins Car," *Automation and Remote Control*, Vol. 82, No. 5, 2021, pp. 745–758, doi:10.1134/S0005117921050015.

[25] Buzikov, M. E. and Galyaev, A. A., "Minimum-time lateral interception of a moving target by a Dubins car," *Automatica*, Vol. 135, 2022, pp. 1–8, doi:10.1016/j.automatica.2021.109968.

[26] Isaacs, R., *Differential Games*, John Wiley and Sons, New York, 1965.

[27] Merz, A. W., *The Homicidal Chauffeur – a Differential Game*, Ph.D. thesis, Stanford University, 1971.

[28] Coates, S., Pachter, M., and Murphey, R., "Optimal Control of a Dubins Car with a Capture Set and the Homicidal Chauffeur Differential Game," *IFAC-PapersOnLine*, Vol. 50, No. 1, 2017, pp. 5091–5096, doi:10.1016/j.ifacol.2017.08.775.

[29] Cacace, S., Lai, A. C., and Loreti, P., "Modeling and Optimal Control of an Octopus Tentacle," *SIAM J. Control Optim.*, Vol. 58, No. 1, 2020, pp. 59–84, doi:10.1137/19M1238939.

[30] Bakolas, E. and Tsiotras, P., "Optimal Synthesis of the Asymmetric Sinistral/Dextral Markov-Dubins Problem," *Journal of Optimization Theory and Applications*, Vol. 150, No. 2, 2011, pp. 233–250.

[31] Berdyshev, Y. I., "Time-Optimal Control Synthesis for a Fourth-Order Nonlinear System," *J. Appl. Math. Mech.*, Vol. 39, No. 6, 1975, pp. 948–956.

[32] Owen, M., Beard, R. W., and McLain, T. W., "Implementing Dubins Airplane Paths on Fixed-Wing UAVs," in "Handbook of Unmanned Aerial Vehicles," Springer, pp. 1677–1701, 2015.

[33] Rubies-Royo, V., Fridovich-Keil, D., Herbert, S., and Tomlin, C. J., "A Classification-based Approach for Approximate Reachability," in "2019 International Conference on Robotics and Automation (ICRA)," , 2019, pp. 7697–7704, doi:10.1109/ICRA.2019.8793919.

[34] Matveev, A. S., Magerkin, V. V., and Savkin, A. V., "A Method of Reactive Control for 3D Navigation of a Nonholonomic Robot in Tunnel-Like Environments," *Automatica*, Vol. 114, 2020, p. 108831, doi:10.1016/j.automatica.2020.108831.

[35] Sultan, M. M., Biediger, D., Li, B., and Becker, A. T., "The Reachable Set of a Drone: Exploring the Position Isochrones for a Quadcopter," in "2021 IEEE International Conference on Robotics and Automation (ICRA)," , 2021, pp. 7679–7685, doi:10.1109/ICRA48506.2021.9561715.

[36] Botkin, N. D., Hoffmann, K.-H., and Turova, V. L., "Stable Numerical Schemes for Solving Hamilton–Jacobi–Bellman–Isaacs Equations," *SIAM Journal on Scientific Computing*, Vol. 33, No. 2, 2011, pp. 992–1007, doi:10.1137/100801068.

[37] Takei, R. and R.Tsai, "Optimal Trajectories of Curvature Constrained Motion in the Hamilton–Jacobi Formulation," *Journal of Scientific Computing*, Vol. 54, 2013, pp. 622–644.

[38] Munts, N. V., "Numerical Study of Different Variants of Dubins' Car Model," in "Proceedings of the 60th Israel Annual Conference on Aerospace Sciences," Tel-Aviv & Haifa, Israel, 2020, pp. 1006–1022.

[39] Zimovets, A. A., Matviichuk, A. R., Ushakov, A. V., and Ushakov, V. N., "Stability Property in the Convergence Game Problem in the Presence of Phase Constraints," *J. Comput. Syst. Sci. Int.*, Vol. 60, No. 4, 2021, pp. 530–548, doi: 10.1134/S1064230721040110.

[40] Cockayne, E. J. and Hall, G. W. C., "Plane Motion of a Particle Subject to Curvature Constraints," *SIAM Journal on Control and Optimization*, Vol. 13, No. 1, 1975, pp. 197–220.

[41] Patsko, V. S., Pyatko, S. G., and Fedotov, A. A., "Three-Dimensional Reachability Set for a Nonlinear Control System," *Journal of Computer and Systems Sciences International*, Vol. 42, No. 3, 2003, pp. 320–328.

[42] Pontryagin, L. S., Boltyanskii, V. G., Gamkrelidze, R. V., and Mischenko, E. F., *The Mathematical Theory of Optimal Processes*, Interscience, New York, 1962.

[43] Lee, E. B. and Markus, L., *Foundations of Optimal Control Theory*, Wiley and Sons, New York, 1967.

[44] Patsko, V. S. and Fedotov, A. A., "Three-Dimensional Reachable Set at Instant for the Dubins Car: Properties of Extremal Motions," in "Proceedings of the 60th Israel Annual Conference on Aerospace Sciences," Tel-Aviv & Haifa, 2020, pp. 1033–1049.

[45] Patsko, V. S. and Fedotov, A. A., "Analytic Description of a Reachable Set for the Dubins Car," *Trudy Instituta Matematiki i Mekhaniki URO RAN*, Vol. 26, No. 1, 2020, pp. 182–197, doi:10.21538/0134-4889-2020-26-1-182-197. (in Russian).

[46] Savelov, A., *Planar curves*, Fizmatlit, Moscow, 1960. (in Russian).

[47] Spiegel, M., *Mathematical Handbook of Formulas and Tables*, Schaum's outline series, McGraw-Hill Book Company, 1968.

[48] Kurnosenko, A. I., "An Inversion Invariant of a Pair of Circles," *Journal of Mathematical Sciences*, Vol. 110, No. 4, 2002, pp. 2848–2860, doi:10.1023/A: 1015310614585.

[49] Filippov, A. F., "An Elementary Proof of Jordan's Theorem," *Uspekhi Mat. Nauk*, Vol. 5, No. 5, 1950, pp. 173–176. (in Russian).

[50] Cairns, S. S., "An Elementary Proof of the Jordan-Schoenflies Theorem," *Proceedings of the American Mathematical Society*, Vol. 2, No. 6, 1951, pp. 860–867.

[51] Filippov, A. F., "On Certain Questions in the Theory of Optimal Control," *J. SIAM Control; Ser. A*, Vol. 1, No. 1, 1962, pp. 76–84, doi:10.1137/0301006.